THE DEVELOPMENT OF A HIGH-THROUGHPUT MICRODROPLET BIOREACTOR DEVICE FOR MICROBIAL STUDIES

A Thesis

by

ADRIAN RYAN GUZMAN

Submitted to the Office of Graduate Studies of
Texas A&M University
in partial fulfillment of the requirements for the degree of

MASTER OF SCIENCE

August 2012

Major Subject: Electrical Engineering

The Development of a High-throughput Microdroplet

Bioreactor Device for Microbial Studies

THE DEVELOPMENT OF A HIGH-THROUGHPUT MICRODROPLET BIOREACTOR DEVICE FOR MICROBIAL STUDIES

A Thesis

by

ADRIAN RYAN GUZMAN

Submitted to the Office of Graduate Studies of
Texas A&M University
in partial fulfillment of the requirements for the degree of

MASTER OF SCIENCE

Approved by:

Co-Chairs of Committee,	Arum Han
	Jun Kameoka
Committee Members,	Jun Zou
	Kenith Meissner
Head of Department,	Costas N. Georghiades

August 2012

Major Subject: Electrical Engineering

ABSTRACT

The Development of a High-throughput Microdroplet
Bioreactor Device for Microbial Studies. (August 2012)
Adrian Ryan Guzman, B.S., Texas A&M University
Chair of Advisory Committee: Dr. Arum Han

Microdroplet microfluidics has gained much interested in the past decade due to its ability to conduct a wide variety of biological and microfluidic experiments with extremely high repeatability on a mass scale. In particular the ability to culture multiple batches of cells by creating microdroplets with a single encapsulated cell and observe their growth overtime allows for specific conditioning of cells. In addition, when conducting co-culture experiment the induction of a certain stimulus may provide observational rare differences in growth that may be characterized by harnessing a single batch of cells out of thousands of samples.

This thesis first presents a variety of microdroplet microfluidic devices that use specific techniques to sufficiently produce, synchronize, merge, and analyze microdroplets. Although many of the devices are capable of producing stable droplets and somewhat efficient synchronization, the overall merging efficiency for most passive or active merging methods alone is lacking. Improvements on such methods and the incorporation of multiple merging methods can lead to a higher overall merging efficiency and greater droplet stability. Also, multiple droplet detection methods can be

employed to analyze cellular growth under different conditions, while passive or active sorting methods can be used to acquire particular microdroplet samples downstream.

The work presented in this thesis entails the characterization and detailed analysis of all aspects of microdroplet microfluidics necessary to adequately produce a microdroplet co-culture device for microbial studies. This includes the incorporation of multiple microdroplet generators for the production of water droplets immersed in oil serving as bio-reactors for cell culture experiments. In addition, multiple microdroplet synchronization devices were tested to sufficiently align multiple trains of droplets for downstream merging using a variety of passive, active, or combination merging methods. In particular, the use of an electric field can cause destabilization of the surfactant surrounding a microdroplet and allow for the formation of a liquid bridge. The formation of this liquid bridge in conjunction with passive merging methods can lead to droplet electrocoalescence. The incorporation of a more uniform electric field that reduces the angle between the droplet dipole moment and E-field can lead to better droplet merging while reducing voltage and frequency requirements observed in previously publications. The testing, observation, and optimization of such aspects of microdroplet microfluidics are crucial for the advancement and production of sound microdroplet culture devices for a variety of applications including the analysis of dangerous pathogenic substances, drug testing or delivery, and genetic studies. Using a newly designed electrocoalescence system we were able to develope a microdroplet bioreactor device capable of merging droplets with a higher efficiency, while using less input requirements.

DEDICATION

To my family and friends for their love and support

ACKNOWLEDGEMENTS

I would like to thank my advisor and committee chair, Dr. Arum Han, for his guidance, support, and mentor-ship. I would also like to thank my committee members, Dr. Jun Kameoka, Dr. Jun Zou, Dr. Kenith Meissner, and Dr. Ji Jim, for their involvement in my academic carrier and willingness to sacrifice their valuable time so that I may continue my education.

I would also like to take this time to thank my collaborators Dr. Figuerido and Dr. Lei for their involvement, including their expertise and supplying of biological cells for testing and incorporation into my devices. Also, I would like to thank my group members and colleagues Jaewon Park, Huijie Hou, Hyunsoo Kim, Chiwan Koo, Osman Cifci, Celal Erbay and Han Wang for their help, patience, and knowledge. Thanks also to the department faculty and staff for making my time at Texas A&M University a great experience.

NOMENCLATURE

E-Field	Electric Field
PDMS	Polydimethylsiloxane
UV-light	Ultra Violet Light
PAA	Peroxyacetic Acid
E.coli	Escherichia Coli
AC	Alternating Current
DC	Direct Current
PCR	Polymerase Chain Reaction
MOS-FET	Metal-Oxide-Semiconductor Field-Effect Transistor
BSA	Bovine Serum Albumin
GFP	Green Fluorescent Protein
RFP	Red Fluorescent Protein
LED	Light Emitting Diode
PMT	Photomultiplier Tubes

TABLE OF CONTENTS

LIST OF FIGURES

1. INTRODUCTION

1.1 Objective and Motivation

Considering the somewhat unknown highly complex genetic microbial interactions present in natural environmental microbial communities, it is necessary to adequately characterize such interactions with high repeatability. Although many current microfluidic methods may be employed to examine such microbial interactions, advances in ultra-high-throughput microdroplet microfluidics provide unparalleled poly-microbial analysis of one-to-one microbe interactions on a mass scale [1]. Droplet microfluidics includes the use of two immiscible fluids such as oil and water to generate identical volumes of one fluid in another [2]. In essence, due to the velocity profile and shear stress induced by a higher oil flow rate, water droplets are cleaved from a steady stream of aqueous solution. Such droplets can be used as bio-reactors for the analysis of cellular cultures, drug delivery applications, co-culture applications, and a wide variety of biological experiments [3]. In order to successfully accomplish the analysis of such cellular communities much work is needed in the optimization and on chip incorporation of a droplet incubation and detection system. The combinatory employment of a fully functional dual microdroplet generation device with one-to-one droplet merging, co-culture, and droplet sorting for the continuous interrogation of specific environmental microbial communities has yet to be performed. This system is capable of

---

This thesis follows the style of *Lab on a Chip*.

simultaneously co-cultivating different microorganisms within hundreds to thousands of droplets with extremely high repeatability. In addition, the incorporation of a microdroplet device capable of analyzing select agents in combination with a target cellular species will provide insight for downstream studies for the characterization of genomic and transcriptomic interactions.

The incorporation of a fully function on-chip microdroplet co-culture system capable of performing all experimental biological functions would be a highly effective tool for biological researchers working with hazardous biological agents. In essence, the ability to conduct conventional biological experiments on extremely dangerous select agents completely on-chip will extremely reduce the possibility of exposure. The device presented in this thesis has the end capability of providing such safety measurements by mass culturing selective agents with high repeatability while being completely encased in a PDMS culture device. In addition, the ability to continuously cycle samples of interest for additional downstream testing or harness particular samples prevents the removal of a selective agent from the device and provides the foundation for evolutionary studies. For instance, the genetic interaction between naturally occurring microbes has shown to provide the crossing of certain genetic material from one species of microbes to another [4]. This interaction can be characterized by co-culturing selective microbes in microdroplet devices and cycling them through the device with a give stimulus to produce already known or possibly unknown species. As one can imagine, there can be an extreme danger in producing such agents, but the complete isolation of such agents within a microdroplet microfluidic device provides an additional

safety barrier for researchers. Also, such devices provide the ability to fully understand microbial interactions and distinguish naturally occurring mutations before they have become prevalent in the environment [5]. In such cases it would be possible to recognize harmful mutations before an epidemic can occur naturally and give researchers valuable time to combat such a crisis that would otherwise not be possible.

1.2 Conventional Microdroplet Microfluidics

Conventional microdroplet microfluidics is characterized by a number of aspects/tools that are necessary to adequately produce a fully functional microdroplet system. Although there are many manipulation based aspects to microdroplet microfluidics with many different techniques to accomplish a variety of tasks, the main aspects include: microdroplet generation, microdroplet synchronization, microdroplet merging, microdroplet detection, and microdroplet sorting [6].

1.2.1 Microdroplet Generation

The effective generation of microdroplets can be accomplished in a number of fashions, but require the use of a more viscous immiscible fluid such as oil and a less viscous fluid such as water or culture media. In most cases it is also beneficial to use a surfactant (suspended in the viscous fluid such as oil) capable of surrounding the microdroplet and creating an additional barrier at the boundary between the water and oil phases [7]. Droplet generation in general can be accomplished using either passive or active methods, which both have their advantages and disadvantages.

Active microdroplet formation methods such as wall chopping can be successful in creating single droplets with extreme control [8]. Two pneumatic compressed air channels can be used on both sides of a straight microfluidic channel creating a two sided valve-like structure [8]. A pre-sheathed flow focused liquid such as water can be generated by creating a cross-junction prior to the wall chopping region that is then restricted by the compression of adjacent wall choppers [9]. The disadvantage to this system is the dependency on a high speed actuation system to generate droplets, limiting the high-throughput potential of microdroplet microfluidics. In addition, the wall chopping schematic requires a precise pressure to provide sufficient constriction of the microfluidic channel for droplet formation and a lack of sufficient pressure may lead to leakage or no droplet formation [10]. Alternatively the high flow speed and control of droplet generation allows for independent manipulation of droplets and precise control for downstream testing [11]. Additional methods include the use of arrays of choppers that vertically collapse a flow-focused liquid within a microchannel, capable of creating multiple droplets with a single actuation [12]. Such chopping methods have also been known to create multi-emulsion droplets where two or more choppers are positioned side by side to create an initial droplet and then a reverse double emulsion [12]. In this instance, an oil droplet would be suspended in water, that is then chopped to create a water droplet with the oil droplet encapsulated inside the water droplet [13]. It has also been shown, that the use of an electric field can be beneficial in the creating of droplets, as the aqueous solution experiences polarization and can be separated from the bulk fluid in the direction of the electric field, producing picoliter volume microdroplets [14].

The most common passive droplet generation method is a conventional T-junction, where a continuous oil phase is used to cleave a perpendicular water inlet into microdroplets [15]. Although such passive methods lack the ability to precisely control or produce droplets the production of droplets is purely dependent on inlet flow speeds [16]. The droplet generation rate of passive methods can far surpass the droplet generation rate of active methods and have the potential to provide extremely high-throughput droplet microfluidic manipulation for downstream experimentation. The formation of water in oil or oil in water droplets can be primarily characterized by the hydrophobicity or hydropholicity of the channel walls [17]. In the case of oil droplets in water a hydrophilic channel wall surface is needed to prevent oil microdroplets from being attracted to the wall surface [18]. Conversely water in oil droplets require the use of a hydrophobic channel such as PDMS to prevent the attraction of water to the wall surface [19]. In addition, it is also beneficial to use a narrower perpendicular channel compared to the continuous phase liquid, which also primarily controls the droplet size. The droplet size is also affected by the perpendicular fluid flow speed (which is usually significantly smaller than the continuous fluid flow speed, 1:3) ratio compared to the continuous fluid flow speed. According to previous experimentation and analysis, the interfacial tension resisting deformation, the tangential shear acting on the interface and the squeezing pressure across the droplet are the primary forces involved in droplet generation [20]. The partial blocking of the continuous phase by the emerging interface creates a pressure difference across the droplet and a difference in the upstream and downstream fluid resulting in droplet formation [21]. It has also been shown that the use

of a magnetic field can aid in inducing the formation of droplets when using a magnetic emerging fluid such as a ferrofluid [22]. Alternative passive microdroplet formation methods include flow focusing or cross-junction emulsion formation devices. Such devices include a simple cross-junction where two opposite inlet fluids, such as oil, cleave a straight flowing fluid, such as water [23]. Flow focusing methods usually include a similar cross-junction structure, but with a narrowing continuous water inlet that provides additional hydrodynamic forces for droplet generation [24]. Alternative methods include the incorporation of 3D capillary droplet makers inserted into a wider continuous flowing tube [25]. In either case droplet formation rate is considered comparable to T-junction droplet generation methods, and both cases are capable of creating multiple emulsions. In addition, the use of air or a completely different substance all together such as polymers, gelatins, or hydrogels have been used to create different substance droplets for downstream manipulation.

In particular, the production of biopolymer droplets is possible using conventional droplet generation methods, and downstream manipulation methods allow the polymerization or harnessing of droplets for future experimentation [26]. For instance, sodium alginate with cross-linker solution can be used to create a downstream gelatin microdroplet [27]. Microdroplet generation can be used for the initial preparation of microparticles that can be exposed to UV-light for polymer cross-linking [28]. Particularly in the case of microgels, poly(N-isopropylacrylamide) can be photo-cured to produce microdroplet hydrogels[29].

1.2.2 Microdroplet Stability in Culture

In many cases the hydrodynamic forces inherent to the substrate surface of microdroplet devices is not enough to sufficiently produce same size droplets. For instance in the case of PDMS devices, although the device is largely hydrophobic there still may be surface interactions with water droplets leading to the incomplete formation or lagging formation of droplets. In microdroplet microfluidic systems the interfacial tension plays a large predominant role in droplet formation, primarily due to the large surface area to volume ratio [30]. In such cases it has been shown beneficial to use a surfactant material to reduce the surface tension of droplets, especially in long term culture instances [31]. A surfactant is generally comprised of a hydrophilic head group and hydrophobic tail group (or converse orientation) that is capable of surrounding a droplet and creating an additional barrier between droplets [32]. In the case where the surfactant is almost the critical micelle concentration (usually 1-3% wt/wt), sufficient droplet surface coverage is observed. Previous experiments have shown that the use of surfactants can reduce droplet to droplet interaction, reducing the diffusion of small molecules from one droplet to another to less than 4% [33]. Although there are many benefits to using surfactants, especially in droplet generation or formation, this provides an additional barrier for downstream droplet manipulation such as droplet merging. Consequently alternative droplet merging methods may be required when attempting to merge droplets that are covered in surfactant proteins.

1.2.3 Microdroplet Synchronization

When considering downstream merging techniques, the proximity of two adjacent droplets is of significant importance. In many passive merging methods, if a pair of microdroplets are separated by too great of a distance, then merging is in some cases impossible. Hence, the synchronization of two trains of droplets is of extreme importance when attempting downstream droplet merging. Considering the different flow speeds of droplets based on their size, it is possible to synchronize a large droplet followed by a smaller droplet provided there is sufficient length for the smaller droplet to catch up to the larger one [34]. This difference in speed is due to the continuous fluids ability to apply the same force perceived by the larger droplet onto the smaller droplet resulting in a faster flow speed [35]. Passive droplet synchronization methods include the use of railroad-like structures joining two adjacent trains of droplets and an oscillator/regulator system for pressure equalization. In the first case, railroad-like structures act as a resistive circuits where droplets present in a segment of the railroad add a resistive component to the constant resistance present in that particular branch of the railroad[29]. Creating an even number of railroad-like structures causes the resistance of perpendicular rails to equal each other in opposite directions leading to an equilibrium state and the synchronization of droplets. Although this method is capable of synchronizing droplets, the synchronization is heavily dependent on the droplet size and flow speeds of the inlet fluids. When the flow speeds are equal and the droplet size is small to moderate droplet synchronization occurs, but when moderate to large droplets

are used the synchronization efficiency is considerably reduced [29]. In addition, the connection of a single railroad-like structure or oscillator in conjunction with an oil regulator that provides additional equilibrium to two trains of droplets has been shown to provide high efficiency synchronization [36]. In particular this system is capable of producing synchronized droplets at lower flow rates and alternating droplets at slightly higher flow rates, making downstream droplet manipulation possible for a variety of applications [36]. Lastly active methods include the use of electrodes to induce an electric field for precise droplet production at 500V [37]. In essence as a droplet passes a pair of electrodes an impedance is observed by the circuit and an adjacent droplet generator connected by the same electrode experiences an increase in the electric field. This causes the production of droplet at the exact same interval the initial droplet is positioned between the initial electrodes [37].

1.2.4 Passive Microdroplet Merging Techniques

Passive merging methods include the use of geometric structures to induce the formation of a liquid bridge and subsequent merging of two adjacent droplets. Although most passive methods have the capability of merging droplets with high-throughput, the use of surfactants greatly hinder the efficiency of such passive methods. The incorporation of surfactants, as mentioned previously, provide additional surface stability and add complexity to the surface tension experienced by microdroplets. The simplest of droplet merging techniques includes the incorporation of a Y-junction or T-junction where two droplets meet at precisely the same time and experience an equalized

deformation [38]. It is shown, that the merging of droplets in this instance in particular is dependent on the flow speed of droplets entering the junction. Low flow rate droplet pairs tend to experience deformation and van der Waals forces for a longer time leading to the thinning of the two interfaces and formation of a liquid bridge [38]. Conversely higher flow rates tend to reduce the amount of time the droplets are in contact and the interfacial energy produced by the squeezing of the two droplets is quickly released preventing droplet merging [39]. It has also been shown that the widening of a channel to slow the droplet movement and decrease the distance between two droplets, followed by the narrowing of the same channel can produce a push-pulling force that induces liquid bridge formation and droplet merging [40]. In such cases the use of surfactant greatly hinders droplet merging and in most cases synchronization is either required or greatly increases the droplet merging efficiency. In addition, as previously mentioned a larger diameter droplet followed by a smaller droplet allows for droplet contact and in conjunction with a serpentine like channel, droplet merging of these two different size droplets is possible [35]. Additional methods include the incorporation of pillar structures that reroute the main flow of oil around a trapped water droplet, allowing for another upstream droplet to make contact with the trapped droplet [41]. In such a case, a similar push-pull force is experienced by adjacent droplets and this deformation causes the formation of a liquid bridge. After droplet merging is induced the increased droplet area causes a decrease in rerouted flow and the removal of the droplet from the pillar array. Again in such cases only the use of a weak surfactants or extremely low concentration surfactants is possible. Alternative methods include the alternation of the

surface properties of the channel surface itself. For instance, the use of PAA to surface coat a PDMS channel and make a small region hydrophilic causes the temporary trapping of a single water droplet [42]. As a second water droplet enters the hydrophilic region the two droplets instantaneously merge and drag force experienced by the much larger droplet causes the removal of the water from the region [42]. Considering oil in water based methods, a hydrophilic surface such of glass would have to be surface treated to create hydrophobic regions for merging of oil droplets. In addition such methods can be used for alternating multi-emulsion processed or manipulation of droplets based on their hydrodynamic forces.

1.2.5 Active Microdroplet Merging Techniques

Considering the inability of most active methods to merge droplets with the use of effective or high concentration surfactants, much research has been conducted to find alternative active merging methods. These methods often produce much larger forces that are capable of overcoming the additional surface stability added by surfactant usage. Single target droplet merging can be accomplished using a laser in a variety of ways including cavitational bubble induction, thermal localized heating, or surface convective heating. In the case of cavitational bubble induction, a bubble containing the vapor of the dispersed phase is induced using a localized laser heating source [43]. The droplet then expands and deforms making contact with an adjacent droplet and upon removal of the laser the bubble then rapidly shrinks causing a push-pulling force and rupture of the film between droplets [43]. This then induces droplet merging using the same principles

experienced by most passive merging methods. In the case of thermal localized heating, a near-infrared light source is used to heat the back-side of a droplet causing thermocapillary effects and convective fluid motion within the droplet [44]. Convective heating causes a drop in density of the organic phase due to an increase in temperature and along with Maragoni convection can induce destabilization of the liquid bi-layer between droplets [44]. It has also been shown that the use of surface convective forces produced by heating the surrounding continuous phase can cause temperature gradients within the droplet and produce droplet merging [44]. Although many of the laser induced merging techniques allow for precise one-to-one droplet merging, these merging methods usually lack the ability to produce high-throughput devices and require expensive equipment.

Electrocoalescence of pairs of droplets requires the induction of an electric field strong enough to destabilize the droplet surface and cause merging of two adjacent droplets. Similar to many active merging methods, the droplets are required to be in close proximity or touching to induce merging. In many cases the electric field requires a large AC power source ranging from 50V-1kV depending on the application and design. In addition it has been shown that the alignment of the droplet dipoles and the direction of the electrical field can lead to higher efficiency droplet merging [45]. In particular the angle between the dipole moment of the droplet and the electric field direction should be no greater than 55 º with the most optimal configuration being 0 º [46]. Many schematics have been proposed depending on the application of the microdroplet microfluidics system such as the use of picoinjectors to pull an adjacent liquid from a reservoir [47]. In

such cases the efficiency of droplet merging is purely dependent on whether the electric field is in the on/off position, but the volume which is extracted from the picoinjector is purely based on the speed of the microdroplet and cannot be precisely controlled. In addition, the use of a charged water phase has been shown to produce sufficient merging under electrophoresis forces in a dielectric liquid [48]. The use of localized electric field systems (LEFs) comprised of multiple short distance array-like electrodes has been shown to provide extremely high efficiency droplet electrocoalescence [49]. Even in cases where droplets are not in close proximity, LEFs are capable of temporarily trapping droplets within the electrode array system until an additional droplet makes contract with the trapped droplet and merging is induced [49]. This is primarily observed when using a very low viscosity continuous oil phase that reduces the shear forces experienced by the water droplet [49]. Considering that most biological applications require the use of surfactants for long-term culture stability, microdroplet electrocoalescence offers a relatively inexpensive and high efficiency method for overcoming surfactant surface stabilization. With the optimization of a one-to-one electrocoalescence merging system, one is capable of reducing the voltage and frequency requirements and consequently the electric field required to induce merging.

1.2.6 Microdroplet Sorting Methods

Microdroplet sorting is a vital tool in downstream collection of specific droplets of interest and includes both passive sorting methods based on microdroplet size, as well as active methods including pneumatic actuation of a perpendicular channel. Passive

methods are usually characterized by the difference in channel outlet dimensions, for instance the use of a reverse T-junction that has different width outlet branches causes the separation purely based on droplet size [50]. The local velocity difference between the two outlet channels causes smaller droplets to enter the closer and narrower channel while larger droplets tend to continue down the wider channel, in turn separating the two droplets [50]. The use of multiple bifurcating junctions can also be used to increase the overall efficiency of microdroplet sorting and a looping region can be included to reduce the dead volume or blockage of a single channel causing unwanted mis-sorting due to a large resistance to flow in either outlet branch [51]. Other passive sorting methods include the use of staggered pillar array structures that alter the normal path of droplets based on their size [51]. Larger droplets experience greater lateral movement due to the greater interaction between pillars and droplets, while smaller droplets experience almost no lateral movement and are eluted from the pillar column relatively unchanged [52].

Active methods generally include the induction of some external force on the channel or droplets themselves to alter the droplets position depending on the microdroplets inherent properties. For instance a simple pneumatic cross-junction can be used in conjunction with a detection system to close one outlet while opening an adjacent outlet [53]. This provides highly efficient and controllable sorting of droplets, but in some cases can limit the high-throughput characteristics that make microdroplet microfluidics attractive. In cases where only a single or a few droplets are attempted to be separated from the main stream of droplets, a pneumatic valve configuration is one of the most optimal methods for effectively sorting droplets [53]. In addition the

incorporation of several branched pneumatic valves can be used in conjunction with an oil inlet spacer to acquire a single droplet of interest or further increase the efficiency of droplet sorting. Alternative methods are present such as the use of a ferrofluid that can be included to flow in parallel with the continuous oil phase [54]. The magnetic properties of the ferrofluid allow for the changing of the ferrofluid from one side of the channel to the complete opposite side with the induction of a magnetic field [54]. This essentially produces a lateral movement of the droplet across the channel allowing for the collection of droplets in different outlet branches. Although this method allows for the mass sorting of droplets the response time and alternating induction of a magnetic field may cause problems when trying to sort a single droplet out of a train of droplets.

1.2.7 Applications of Microdroplet Microfluidic Systems

With the advancement and optimization of microdroplet microfluidic techniques pertaining to microdroplet manipulation, the application for droplet microfluidics is drastically increasing. The ultrahigh-throughput capability of microdroplet microfluidics especially when considering biological or cellular culture has shown to considerably decrease the reaction time and reagent consumption when compared to conventional methods [55]. In addition the use of microdroplets as a bio-reactor system for isolated cell growth on a mass scale has proven beneficial in genetic applications such as gene transcription, protein expression, and PCR [56]. Addition applications include the incorporation of selective agents such as drugs in conjunction with cells or other agents to observe drug reactions with high repeatability. In particular, the use of microdroplet

microfluidics for the co-culture of microbial communities for the observation of rare mutation has recently gained our interest [57]. This provides the foundation for future studies presented in this thesis as well as the basis for future works including the potential for completely on-chip integrated microdroplet evolutionary studies.

2. MICRODROPLET MICROFLUIDIC SYSTEM

2.1 Design and Fabrication of Microdroplet Generator

The design of a microdroplet generator is the first key aspect to creating a fully functional microdroplet microfluidic system. The PDMS channel layer is bonded on top of a thin PDMS coated glass slide (Figure 2.1). The design used throughout the majority of this study (with exception to the droplet synchronization system) uses a T-junction droplet generator with a 100µm wide oil inlet and 80µm wide water inlet (Figure 2.2a). In addition to characterize the microdroplet production a series of experiments were conducted using varying flow rates for the oil and water inlets, producing different size droplets at varying frequencies. The basic microdroplet design is similar to the microdroplet culture system previously produced by Park *et al.,* where the T-junction microdroplet generator is followed by a small culture chamber (2.2b: 3mm x 10mm culture chamber) [58].

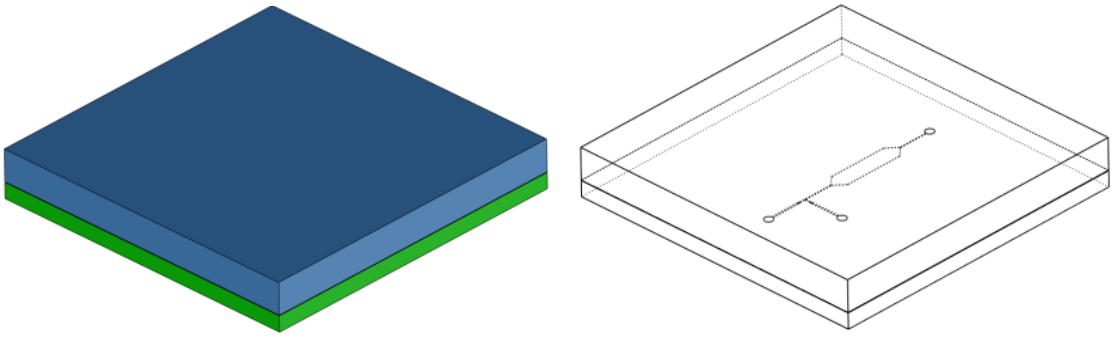

Figure 2.1. 3D model microdroplet culture device. Fabricated microdroplet generator device with spin-coated glass layer (green) bonded to a thick PDMS channel layer (Blue).

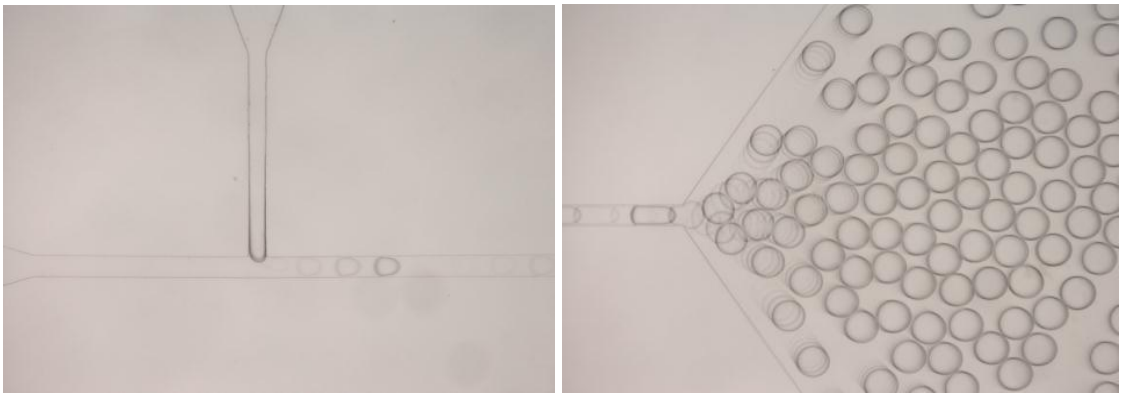

Figure 2.2a, 2.2b Microscopic images of droplet generation. a) Shows a 100µm wide channel for continuous oil phase (from left side) and 80µm wide channel for the water phase (from top). b) Shows downstream 3mm x 10mm culture chamber with 100µm inlet.

The droplet diameter was measured in the culture chamber at each varying flow speed and used to characterize the droplet production (Figure 2.3 & 2.4a & 2.4b) Later synchronization droplet generator systems incorporate a cross-junction droplet generator schematic with a 100µm wide straight water inlet and two perpendicular 50µm wide oil inlets (Appendix A).

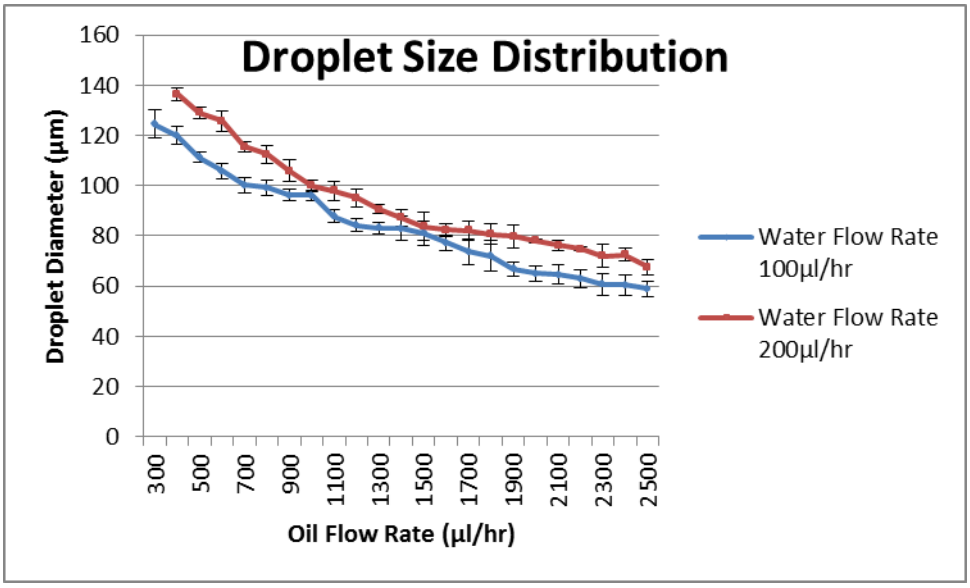

Figure 2.3. Graph microdroplet diameter depending on flow rate. Droplet size distribution depending on varying oil flow rates ranging from 300µl/hr to 2500µl/hr, and water flow rates of 100µl/hr and 200µl/hr. For sufficient droplet generation the water flow rate was required to be less than the oil flow rate, with better droplet generation at ratios of 1:3 or greater respectively.

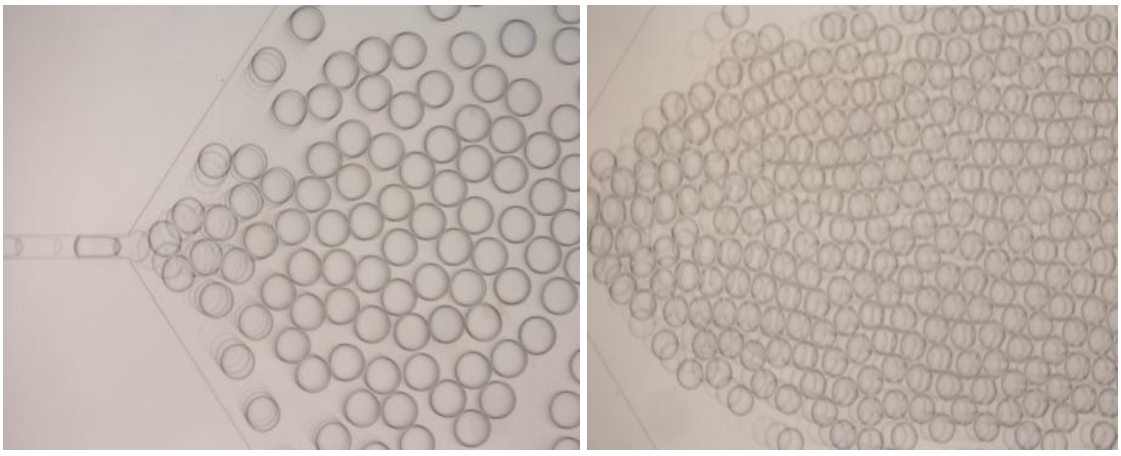

Figure 2.4a & 2.4b. Microscopic images of different flow rate droplets. a) Droplet generation at flow rates of 100µl/hr and 1000µl/hr for water and oil phases respectively. b) Droplet generation at flow rates of 100µl/hr and 2500µl/hr for water and oil phases respectively.

2.1.1 Experimental Testing of Surfactants

Considering the importance of surfactant use for long term droplet stability and downstream cell culture applications, it is necessary to characterize a variety of surfactant materials to determine the most suitable for future culture experiments. Wu *et al.* showed that the use of Span 80 or Tween 20 can increase the surface stability and reduce the surface tension of microdroplets leading to greater long term stability. In this case mixing 2% wt/wt of Span 80 or Tween 20 into the oil phase provides sufficient droplet stabilization [60]. Alternatively the use of Pluronic F108 in the water phase has been shown to produce addition stability with similar but opposite hydrodynamic forces. In particular when using a hydrophilic device such as glass, oil droplets in water can be generated and Pluronic F108 can be used to stabilize these oil droplets. Our application includes the use of water droplets in oil, hence we started by tested the droplet stability of 2% wt/wt Tween 20 in oil. Although previous results show the successful generation of droplets using Tween 20, we found that the surfactant was not strong enough for downstream culture, and upon entering the culture chamber droplets readily merged (Figure 2.5a). Conducting the same experiment with Span 80 we observed sufficient droplet stability and even after an extended culture period droplets were still separated (Figure 2.5b). Although the use of Span 80 produced successful results, the long term culture tended to produce debris material that we attribute to the shear stress experienced at the interface of the droplet. In some instances this may be due to Span 80 forming micelles although the surfactant concentration is expected to be below the critical

micelle concentration. Consequently we attempted to pursue the formation of droplets using a well-known surfactant produced by Evonik® called Abil EM90. Testing the long term stability of this surfactant we found there was a significant reduction in debris material even at relatively high shear stress conditions, in turn the remainder of the experiments presented throughout this thesis use Abil EM90 as the primary surfactant (Figure 2.5c).

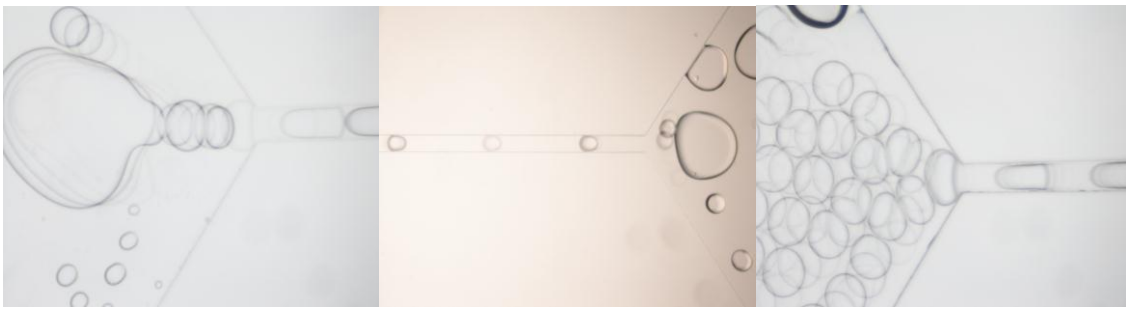

Figure 2.5a, 2.5b & 2.5c. Microscopic images droplet production using different surfactants. a) Droplets produced using no surfactant merge immediately when entering the culture chamber. b) Droplets produced with 2% wt/wt of Tween 20 are somewhat more stable, but merging is still readily observed when droplets make contact at high flow rates. c) Using 2% wt/wt of Abil EM90 in oil produces droplets that are extremely stable even when making contact at high flow rates.

In future experiments we also attempted to encapsulate polystyrene beads inside of microdroplets to observe the culture difference of cells, and in such cases we found it beneficial to use Abil EM 90 at 2% wt/wt in oil and Pluronic F108 2% wt/wt in culture media (Figure 2.6a-2.6d). The use of Pluronic F108 reduced the surface attraction between the hydrophobic polystyrene bead and the hydrophobic PDMS channel wall,

which we attribute to the ability of Pluronic F108 to coat polystyrene beads leaving a hydrophilic surface around the beads that reduce hydrodynamic forces in culture media.

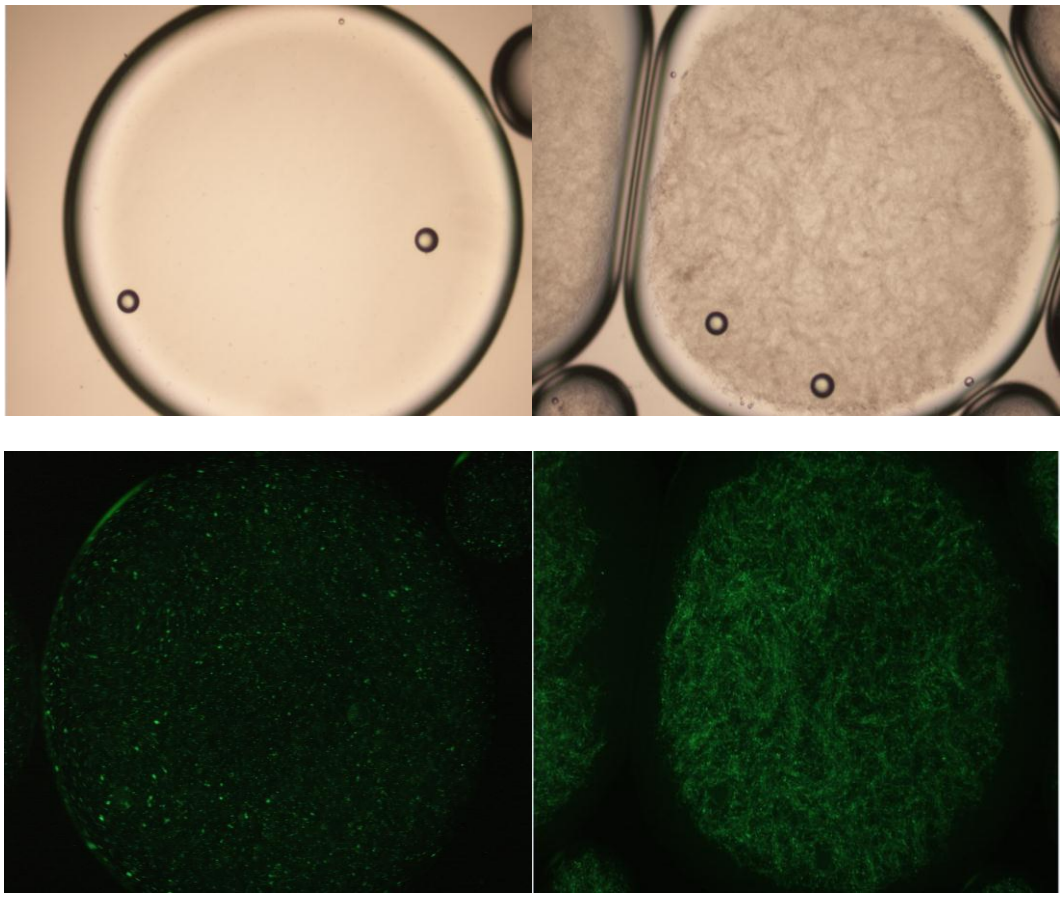

Figure 2.6a-2.6d. Microscopic and fluorescent images of E.coli and particle encapsulation. a) Droplet generation using 2% wt/wt Abil EM90 in the oil phase and 2% wt/wt Pluronic in culture media (top left) b) Fluorescent image of GFP labeled E.coli at time 0 (bottom left) c) Same droplet after 24hr culture (top right) d) Fluorescent image of GFP labeled E.coli at t=24hr (bottom right) showing droplet stability and cell viability even after extended culture periods.

2.1.2 Droplet Stability Testing

When culturing cells for extended periods or repeating cycles it is important to characterize the growth behavior of cells in a confined environment. Although additional culture media can be added or exchanged in the case of cyclic culturing, the growth behavior of a confined microbe may differ from the growth behavior in the natural environment. We created a multi-valve multi-chamber microdroplet device using standard soft-lithography techniques. The initial channel layer is fabricated using a SU-8 master spin coated with PDMS. The previously cured PDMS valve layer is then plasma bonded on top of the channel layer to provide pneumatic actuation of the 4 chambers (Appendix A). The PDMS valve layer is bonded on top of the PDMS channel layer that is then bonded on top of a thin PDMS coated glass slide (Figure 2.7). All additional stability testing is carried out using the multi-valve multi-chamber device to reduce unwanted back pressure that typically causes droplet deformation during extended culture experiments. Essentially 3 chambers can be used as culture chambers, while the last chamber is used for relieving pressure and waste. Using fluorescently labeled E.coli we can observe and characterize the difference in growth by taking fluorescent intensity measurements of a normal petri dish culture and microdroplet culture to compare the growth behavior. Analysis of all fluorescent intensity images is conducted using image j software with a set threshold for each image, where the fluorescent intensity of cells is derived by removing the background noise providing the pure intensity of cells. Using these methods we are able to observe differences in growth rates of cellular cultures .

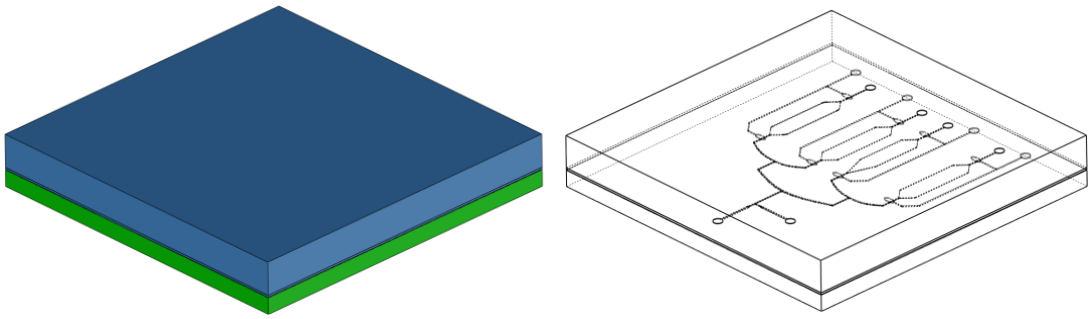

Figure 2.7. 3D model multi-valve multi-chamber microdroplet culture device. Fabricated multi-valve multi-chamber device with spin-coated PMMA slide (green) a thin spin-coated PDMS channel layer (between green/blue) and a thick PDMS valve layer (blue).

While culturing cells using the multi-valve multi-chamber design, we observed the decrease in droplet size during extended cell culture experiments. Consequently we decided to characterize the overall decrease in droplet size during a normal culture (Figure 2.8). Due to the relatively large decrease in droplet size, additional investigation was necessary to determine the exact cause of droplet reduction during culture. In turn, droplets of a known size were created and cultured in a sealed test tube at room temperature conditions and upon analysis of the droplets it was found that the droplet size was relatively constant during a 24 hour culture.

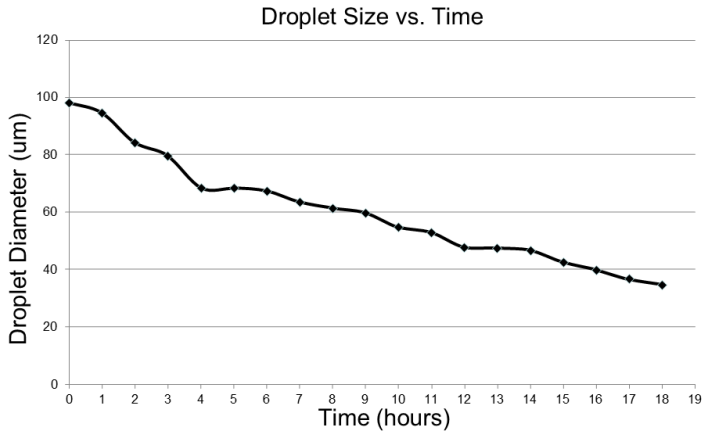

Figure 2.8. Graph droplet size decrease overtime. Droplet size reduction during an 18 hour culture, attributed to PDMS's ability to absorb or allow evaporation of small molecules such as water.

In lieu of this observation, we attribute the reduction in the droplet size to the ability of PDMS to absorb water or allow diffusion of small molecules such as water to the atmosphere [61]. Attempting to counteract the diffusion of water out of the droplets we conducted underwater cultures where PDMS devices were submerged in deionized water for 24 hours prior to culture (Figure 2.9a & 2.9b). In addition, the entire culture was conducted underwater, but in such cases the droplet size was in some cases increased significantly leading to droplet deformation. Droplets initially 80µm in diameter were observed to increase to 100µm during a 24 hour underwater culture experiment. Additional experiments were conducted using a sealed humid environment to simulate a humid incubator environment, which produced only marginal changes in droplet size (Figure 2.10a & 2.10b). Under the humid environment conditions droplets were observed to decrease from 80µm to 78µm, leading us to believe cellular culture is most optimal in a humid environment.

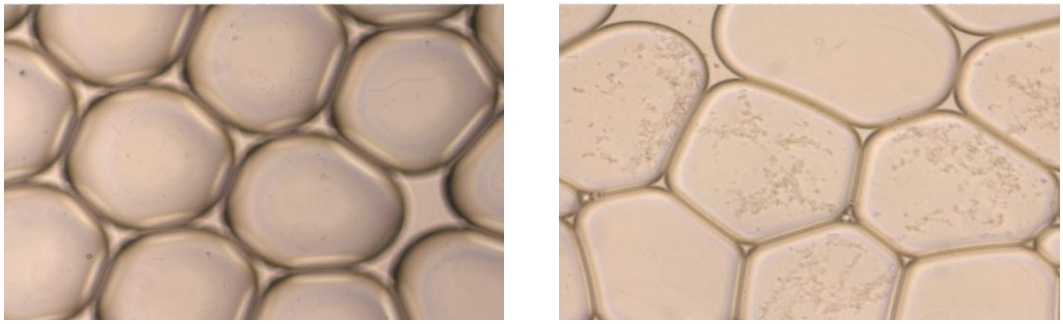

Figure 2.9. Microscopic image underwater culture. a) Initial droplet before submerging culture (80µm). b) Droplets size increase during 24 hour culture of submerged multi-valve multi-chamber device (100µm).

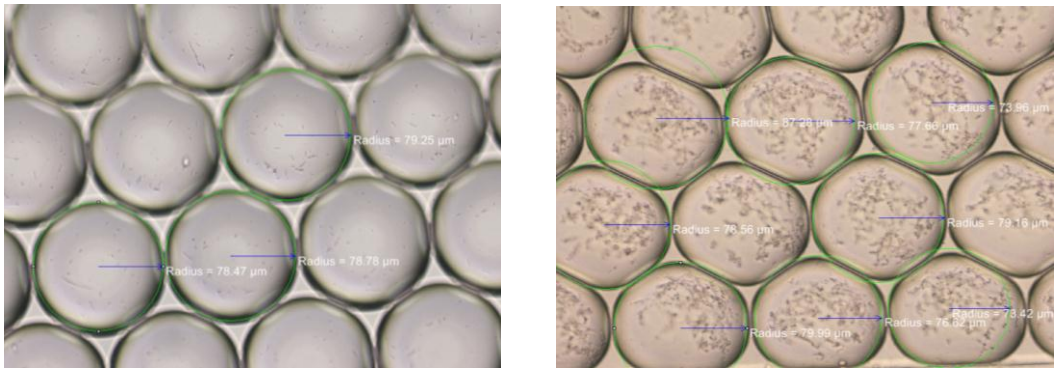

Figure 2.10. Microscopic image humid environment culture. a) Initial droplet before humid environment culture. b) Showing droplet size after 24 hour humid culture experiment.

2.2 Microdroplet Synchronization Design and Fabrication

2.2.1 Testing Railroad-Like Structure

As previously mentioned droplet synchronization is a critical aspect necessary for sufficient downstream droplet merging, especially when using conventional and practical passive or active merging methods. Considering the inert high-throughput

capabilities of microdroplet microfluidics, active methods such as laser convective heating or pneumatic actuated merging may limit such capabilities. The two droplet methods incorporated in our designs were proposed by Ahn *et al.* and Hong *et al.*, which are comprised of railroad-like structures or a pressure oscillator and oil regulator system respectively [36]. All synchronization devices were fabricated using standard soft-lithography process with droplet generators presented previously, followed by a synchronization region (Appendix A).

The railroad-like structure includes two droplet generation inlets 100μm wide, with the two trains of droplets separated by 180μm long railroad crossings. The width of each railroad track was 80μm with the distance between each railroad track being 240μm (Figure 2.11). The dimensions of the entire schematic are directly proportional to previously proposed designs. The synchronization PDMS channel layer is bonded on top of a thin PDMS coated glass slide (Figure 2.12).

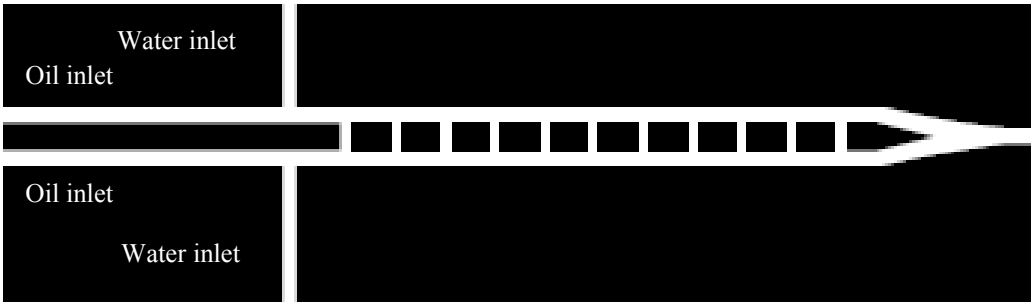

Figure 2.11. Microdroplet railroad-like synchronization design. Railroad-like region of synchronization device.

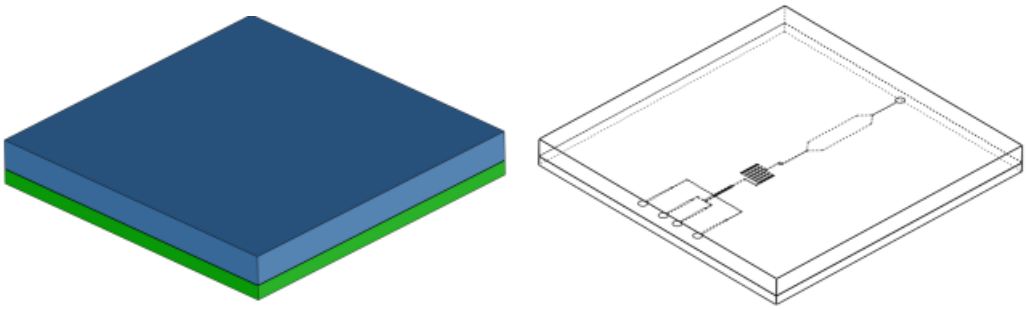

Figure 2.12. 3D model of microdroplet railroad-like synchronization device. Fabricated railroad-like synchronization device with PDMS spin-coated glass layer (green) and thick layer PDMS channel layer (blue).

2.2.2 Testing Oscillator and Regulator System

The oscillator and regulator device is comprised of two cross-junction droplet generators connected by a droplet oscillator that is a single railroad crossing. The dimensions of the water and oil phases are 100µm and (2) 50µm channels respectively. The droplet oscillator is spaced 200µm from the oil inlet and is 100µm wide and is capable of reducing pressure differences between the two symmetric droplet generators (Appendix A). Downstream an additional oil inlet 50µm wide is used as an oil regulator that can further reduce pressure differences in the two trains of droplets by adding an external pressure source so that when a certain resistance is observed by the regulator, flow begins to slow in that branch while the opposite regulator experiencing no resistance has an increase in flow (Figure 2.13). This leads to further synchronization of the two trains of droplets and preparation for downstream manipulation of droplets

including passive or active merging techniques. The oscillator/regulator PDMS channel layer is bonded on top of a thin PDMS coated glass slide (Figure 2.14).

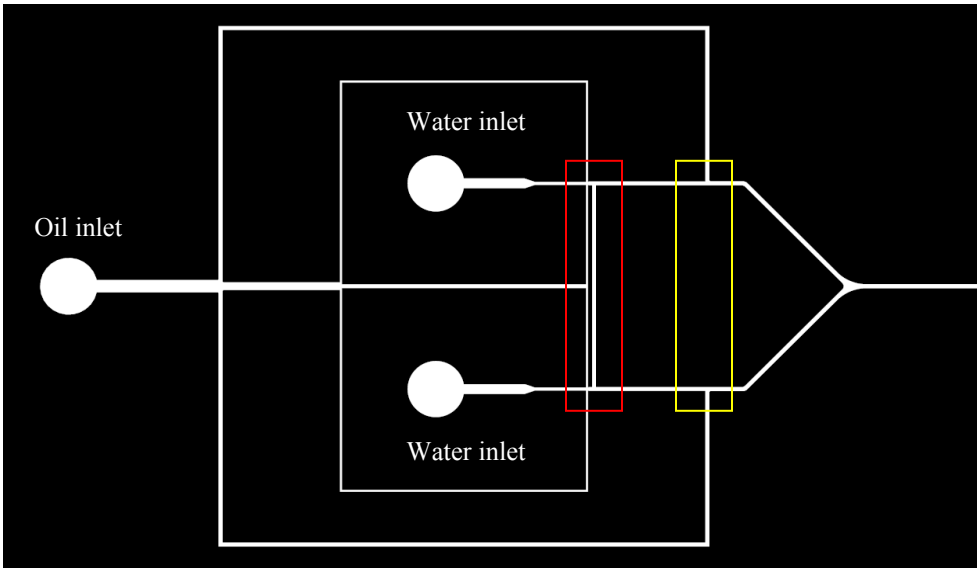

Figure 2.13. Microdroplet oscillator/regulator synchronization design. Droplet oscillator (red) and oil regulator system (yellow).

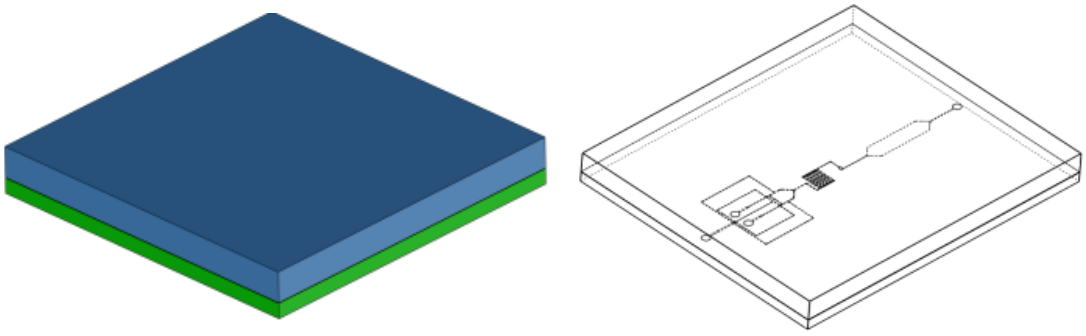

Figure 2.14. 3D model of microdroplet oscillator/regulator synchronization device. Fabricated oscillator/regulator synchronization device with PDMS spin-coated glass layer (green) and thick PDMS channel layer (blue).

2.3 Microdroplet Merging Design, Fabrication, and Testing

2.3.1 Testing Passive Merging Techniques

The main passive merging method used for droplet merging includes the widening of a channel followed immediately by the narrowing of the microfluidic channel. This essentially causes a large difference in flow speed within the widened-narrowed region, in turn producing a push-pulling force that induces a liquid bridge. For our experimental purposes the widened and narrowed channels are scaled according to previous passive merging schematics with later modifications including a 75μm narrowing region prior to a 150μm widened region and 75μm narrowing channel [18](Figure 2.15). When considering passive merging methods, the deformation of droplets and rapid movement while remaining in direct contact with adjacent droplets is crucial for high efficiency merging. Although such methods have shown to produce merging, the merging efficiency is heavily dependent on the lack of surfactant usage and droplet synchronization. In our experiments using Abil EM90 at 2% wt/wt in the oil phase, passive droplet merging efficiency was well below 30%, hence additional merging methods were pursued.

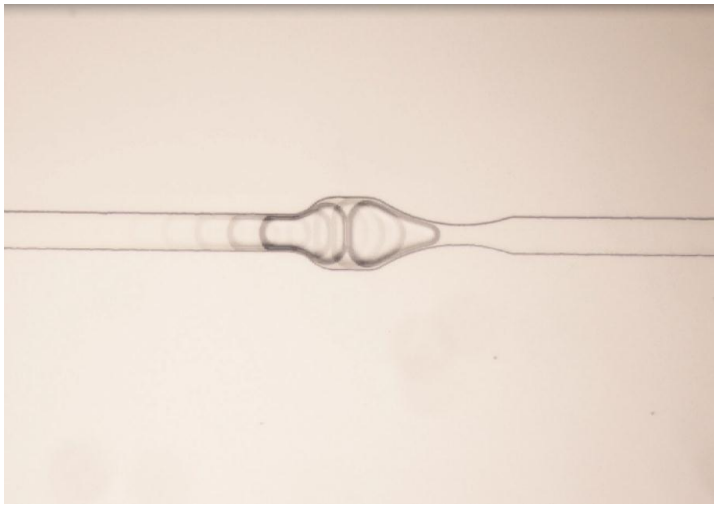

Figure 2.15. Microscopic image of widened/narrowed passive merging device. Widened and narrowed passive merging design.

Pillar array structures have also been used to induce temporary droplet trapping and with the arrival of a second droplet are capable of producing droplet merging. The design experimentally tested in this work entails the widening of a 100µm channel to 300µm, divided by two rows of pillars. The pillars are 20µm wide with increasing vertical lengths, from 20µm to 70µm, as they continue down the length of the channel (Figure 2.16). This produces an increase in flow in the outer pillared channels and allows for the droplet to remain at the last pillar until additional droplets are introduced into the structure. As with other passive merging methods the incorporation of surfactant reduces the droplet merging efficiency to 30-40%. In addition observational experimentation shows that this device is more beneficial for merging multiple droplets or droplets significantly larger than normal droplets produced for a 100µm droplet generator.

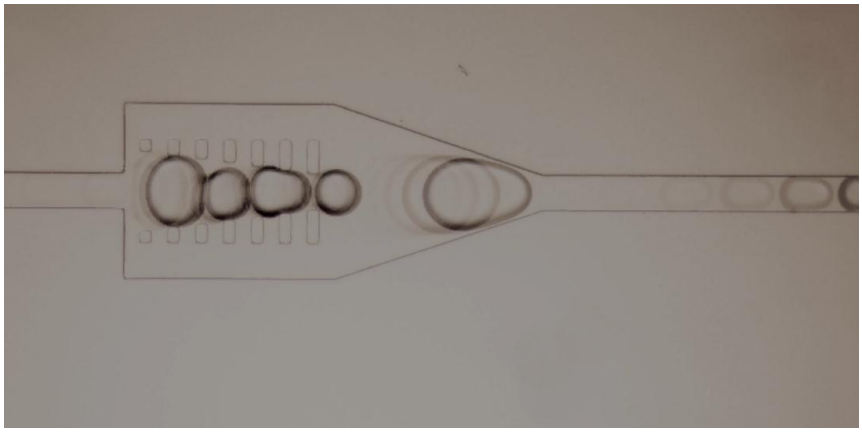

Figure 2.16. Microscopic image of pillar array passive merging device. Pillar array passive merging structure.

2.3.2 Testing Electrocoalescence Devices

2.3.2.1 Experimental Setup: Induction E-Field

Considering the benefits of using surfactant for stable droplet generation and long-term cell culture, active merging methods such as electrocoalescence were pursued for offering high-throughput capabilities with high efficiency. Electrocoalescence includes the use of an external AC power supply to induce a localized electric field in the direction of the droplet movement. It has been shown that the alignment of two adjacent droplet dipole moments and the electric field can lead to destabilization of the droplet surface and instantaneous merging. This requires the use of a high voltage AC power supply, but for our purposes and experimental setup, a pulsed DC signal is used as a high voltage supply source. Acquiring a mos-fet relay (Omron® G3VM-601BY) we were able to use a function generator to control the frequency of a square wave signal that can be relayed to a high voltage DC power supply (Appendix D). A 1V square wave signal is

introduced into the mos-fet relay and the 20mV output signal is observed using an oscilloscope. The DC power supply is then put in series with the mos-fet relay and the electrocoalescence device to produce a 300V-1000V and 0-1.7kHz pulsed signal that acts as a high voltage AC power supply. Upon application of the electric field a noticeable difference in droplet merging is observed, proving the viability of our circuit and induction of the desired electric field. (note: when making comparisons to other electrocoalescence works there may be differences in results depending on the power source used)

2.3.2.2 First Generation Electrocoalescence Device

First generation electrocoalescence devices are created using typical soft-lithography to create the patterned channel layer and wet etching to create the patterned electrodes separately. The SU-8 master is used to create a PDMS channel layer and then is oxygen plasma bonded to a previously PDMS spin-coated electrode layer (Appendix B). The PDMS channel layer is bonded on top of a thin PDMS coated glass slide with two copper electrodes patterned on the surface (Figure 2.17). In order to characterize the necessary vertical lengths needed for sufficient droplet merging, four similar droplet merging devices are created with vary electrocoalescence regions (250µm, 500µm, 750µm, and 1000µm) (Figure 2.18). In addition, all electrodes were patterned using the same mask which has a 500µm wide tip capable of creating a uniform electric field within the droplet merging chamber (Appendix A). It was observed that the 250µm and 500µm length channels did not align the dipole moment of the droplets and electric field

for a sufficient enough time to induce droplet merging. Alternatively droplet merging was observed in the 750µm and 1000µm length electrocoalescence devices, but with varying efficiencies of approximately 50%. Considering this additional devices were designed to characterize the droplet behavior and best schematic for high-throughput droplet merging.

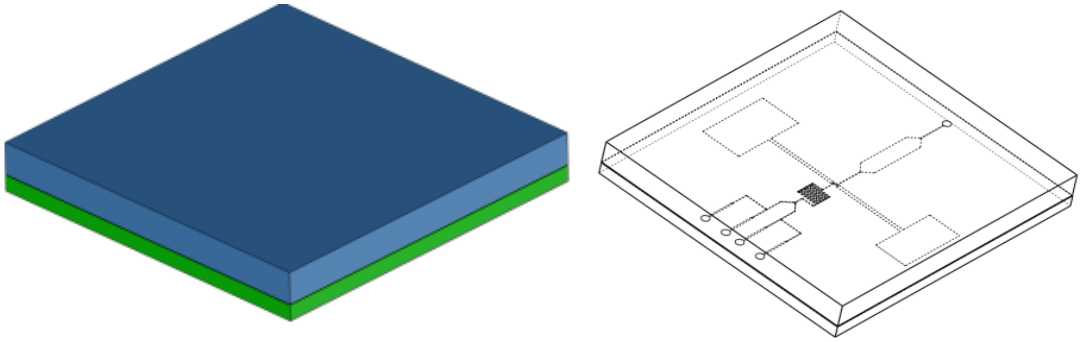

Figure 2.17. 3D model of planar electrocoalescence device. Fabricated planar microdroplet electrocoalescence device with spin coated PDMS on electrode patterned glass (green) and thick PDMS channel layer (blue).

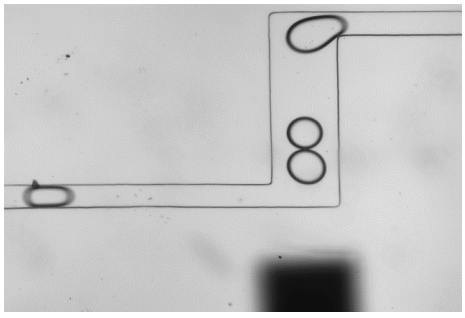

Figure 2.18. a) Microscopic image of planar electrocoalescence device. Droplet merging chamber 750µm long.

2.3.2.3 Passive and Active Merging Combination Device

Attempting to increase the electrocoalescence efficiency a new batch of devices were created that increased the width of the merging channel to 300µm while keeping the length at 750µm and 1000µm. This essentially serves as a widening region for droplets to slow and reduce the distance between adjacent droplets. In addition a narrowing region was incorporated prior to the droplet merging region to induce a push-pulling force similar to that of passive droplet merging methods (Figure 2.19). The combination of passive merging and active electrocoalescence merging is capable of increasing the overall efficiency of the device.

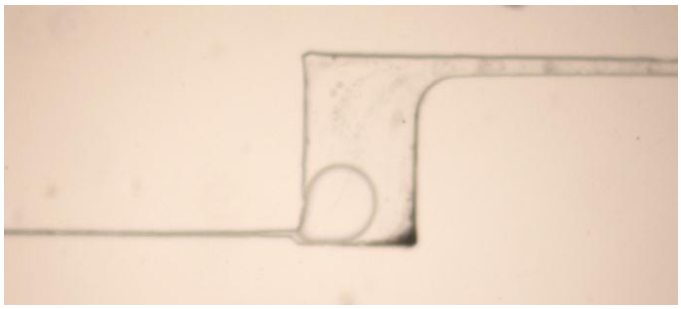

Figure 2.19. a) Microscopic image of second generation electrocoalescence device. Widened droplet merging chamber of 300µm and 750µm long, and narrowed region prior to merging chamber 25µm wide.

2.3.2.4 Co-planar Electrocoalescence Device

Considering conventional electrocoalescence is conducted using a single planar electrode surface, it is also assumed that the use of a co-planar more advanced electrode designs can lead to a better merging efficiency with less voltage and frequency requirements. Hence, a co-planar device is fabricated by plasma bonding a single electrode on the bottom of the spin-coated thin layer PDMS and plasma bonding the

opposing electrode on the top surface of the PDMS channel (Figure 2.21). The PDMS channel layer is sandwiched between two thin PDMS coated glass slide with a single electrode patterned on each (Figure 2.20). This causes the electric field to be diagonally across the droplet merging chamber and should reduce the overall angle between the droplet dipole moment and electric field, leading to better merging efficiency (Appendix D). It was observed that using this configuration droplet merging at a range of voltage and frequencies could reach above 80% efficiency, but with the requirement of a high voltage input of at least 500-900V is required. In addition, when compared to the planar electrode design, droplet merging efficiency was slightly decreased due to the expected electric field orientation not being in line with the overall dipole of the droplets.

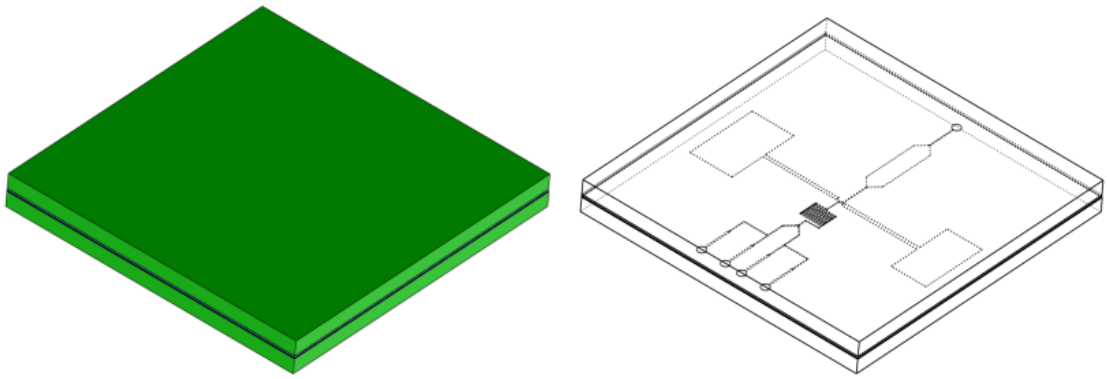

Figure 2.20. 3D model of co-planar electrocoalescence device. Fabricated co-planar electrocoalescence device with two PDMS spin-coated electrode patterned glass slides (green) and a thin PDMS spin-coated channel layer (blue between green)

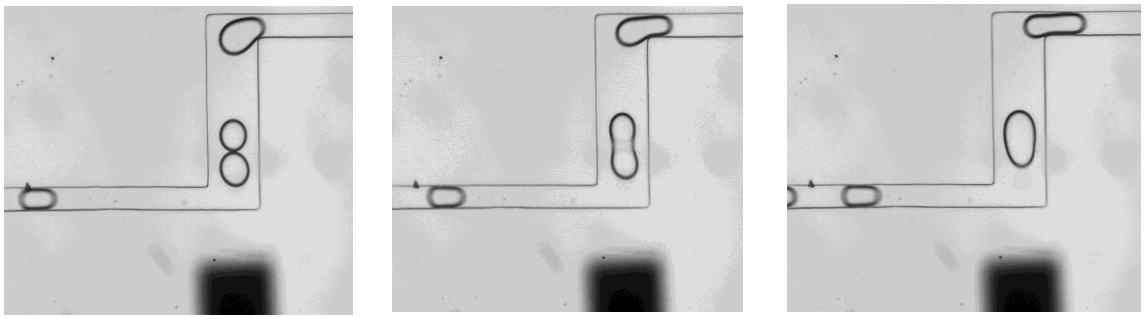

Figure 2.21. Sequential microscopic images of co-planar electrocoalescence device. Droplet merging of synchronized droplets using combination merging methods.

2.3.2.5 Dual Co-planar Electrocoalescence Device

Although previous devices show relative high efficiency with high-throughput droplet production, the voltage requirement for these devices can be improved. Considering this dual-planar electrodes were fabricated using the same mask design used to create conventional planar electrodes, allowing for co-planar positive and co-planar grounded electrodes to produce a much more uniform electric field in relation to the microdroplet dipole moment (Appendix D). The PDMS channel layer sandwiched between two thin PDMS coated glass slide with two electrodes patterned on each (Figure 2.22). Essentially a normal planar electrode device is fabricated using a thin PDMS channel layer, and an additional glass planar electrode is oxygen plasma bonded on the top surface of the microchannel layer (Figure 2.23).

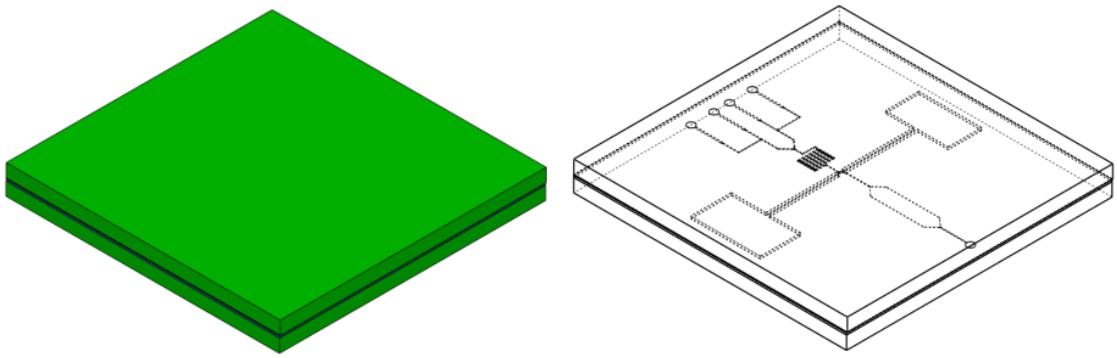

Figure 2.22. 3D model of dual co-planar electrocoalescence device. Fabricated dual co-planar electrocoalescence device with two PDMS spin-coated electrode patterned glass slides (green) and a thin PDMS spin-coated channel layer (blue between green)

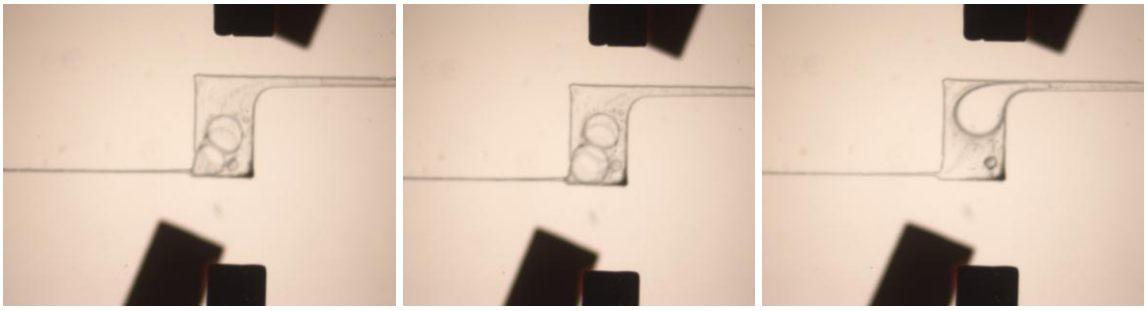

Figure 2.23. Sequential microscopic images of dual co-planar electrocoalescence device. Droplet merging of synchronized droplets using dual co-planar device.

2.3.2.6 Electroplated 3D Electrocoalescence Device

Since the electric field is the driving force for droplet merging in microdroplet electrocoalescence devices, we developed a 3D electrode electrocoalescence device by electroplating a copper electrode seed layer to produce a 100µm high electrode pattern. Using conventional oxygen plasma bonding methods we fabricated the 3D electrocoalescence device with the electrodes cut out of the PDMS channel layer

(Appendix A). The PDMS channel layer is bonded on top of a thin PDMS coated glass slide with two 100µm high electrodes patterned on the surface (Figure 2.24). The use of 3D electrodes will undoubtedly produce the most uniform field in all portions of the microdroplet leading to complete alignment of the dipole moment within the droplet and the electric field. A comparison of each of the devices is conducted by taking a time-lapse image of the merging devices at varying voltage and frequencies to observe the minimum threshold voltage required for droplet merging. In addition the droplet merging efficiency is calculated by comparing the number of droplet pairs merged to the number of non-merged droplets at each voltage/frequency (Figure 2.25).

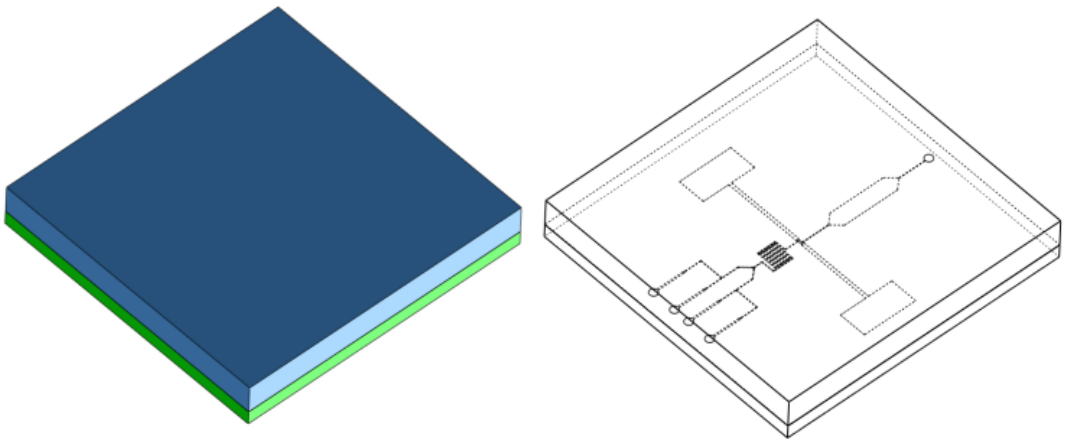

Figure 2.24. 3D model of 3D electroplated electrocoalescence device. Fabricated 3D electrocoalescence device with 100 µm electroplated electrode glass slide (green) and a thick PDMS channel layer (blue).

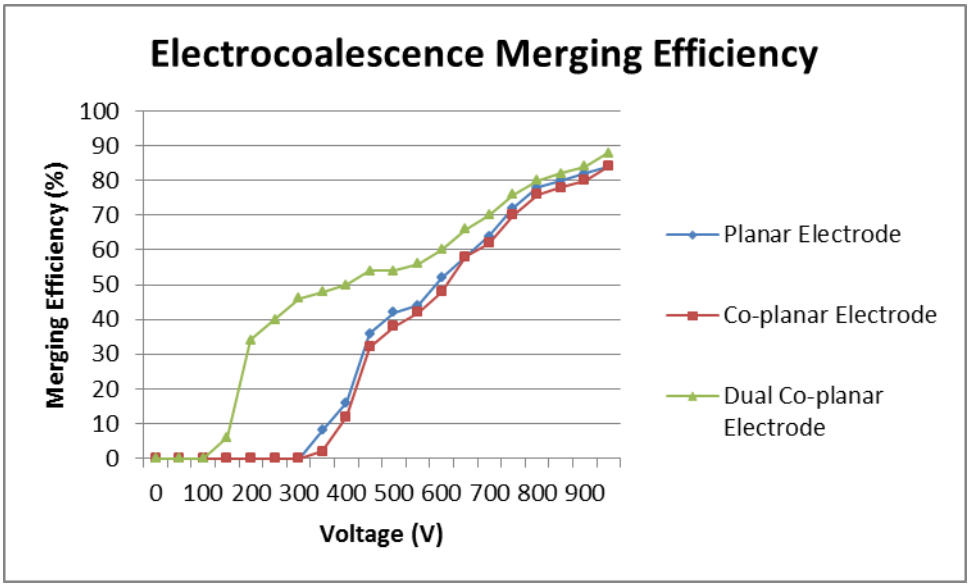

Figure 2.25. Graph comparing the overall merging efficiency of electrocoalescence devices. Including: planar electrodes, co-planar electrodes, dual-coplanar electrodes, and 3D electrodes.

3. SUMMARY AND FUTURE WORK

3.1 Summary

In this thesis, a robust high-throughput microfluidic microdroplet co-culture device was developed to characterize the growth behavior of microbes under certain culture conditions. In addition the work presented provides for the foundation of future studies pertaining to microbial growth and genetic cross-linking naturally observed in the environment.

Several microfluidic microdroplet principles were critically tested and used to optimize the microdroplet device. Multiple surfactants were used to observe the effects on droplet generation as well as the use of surface coating treatments such as BSA or Aquapel for hydrophobic surface coating of syringes and tubing or PDMS respectively. In addition both cross and T-junction microdroplet generation devices were fabricated comparing the difference in generation using Abil EM90 surfactant. The droplet synchronization proved to be a vital tool in providing high efficiency downstream merging using either passive or active merging methods. Several passive merging methods were tested to characterize the merging efficiency, but the overall efficiency was relatively low resulting in a maximum of 50% merging. Alternatively several electrocoalesence devices were fabricated and tested, increasing the overall merging efficiency with each iteration of devices, ultimately reaching an efficiency above 90%.

3.2 Future work

3.2.1 Microbial Co-culture Experiment

3.2.1.1 Experimental Setup

An entire microbial co-culture device is fabricated including all previously mentioned aspects of microdroplet microfluidics (Two droplet generators, a synchronization region, a droplet merging region using electrocoalescence, a chaotic mixing region, and a culture chamber). The device is capable of merging two fluorescently labeled microbes and co-culturing the cells under different culture media conditions to produce specific growth behaviors. Similar to previous works by Park *et al.* microbe behavior can be characterized by growth conditions, serving as the basis for future evolutionary studies pertaining to environmental microbes.

3.2.1.2 Microbe Preparation GFP and RFP

Two sets of microbes are designed having GFP- and RFP- labels which can be distinguished in culture using fluorescent imaging. Initially the concentration of microbes is measured using a hemocytometer measurement and then a necessary dilution is administered based on the concentration and volume of the original sample and the average volume of microdoplets. This will allow us to create droplets with no more than one microbe per droplet, which makes a one-to-one microbe interaction possible upon merging of the two bioreactors. According to Poisson's ration we expect that 1/3 of the droplets will not have any microbes present, but these droplets will not show any fluorescent intensity and will not affect our intensity measurement. After merging

droplets will either have no microbes, a X microbe, a Y microbe, or both microbes. Again the ratio of each droplet is a function of Poisson's ratio depending on the initial droplet production. Hence, adding XX culture media will lead to the growth of X microbes, while YY culture media will lead to the growth of Y microbes. Conversely the addition of XXYY culture media can allow for the growth of both microbes and a difference in growth can be observed using fluorescent intensity measurements. This will characterize the interaction of microbes with one another and provide researchers valuable information about microbe interaction in natural environments.

3.2.1.3 Fluorescent Intensity Measurement and Characterization

The fluorescent intensity is calculated using image j as mentioned previously, by applying a certain threshold and removing background noise to produce the pure intensity of cells in a certain field of view. This allows for the mass characterization of individual droplets or a mass array of droplets, keeping the high-throughput aspects of the microdroplet device intact. Comparing the fluorescent intensities of each culture condition provides a standardized characterization.

3.2.2 Optical Detection System

An optical detection system will provide a mechanism for detecting rare mutations or abnormal growth in a particular droplet and lead to the downstream sorting of microdroplets. The optical detection system will most likely be comprised of two main portions: an LED/PMT system for the specific characterization of differences in growth,

and an optical fiber for initial location detection and sorting. This system can provided on demand detection and pneumatic sorting of droplets based on intensity measurements.

3.2.3 Microdroplet Sorting System

A microdroplet sorting system is necessary to harness the rare growth or mutated cells present during future evolutionary studies of co-cultured microbes. This will most likely be comprised partially of the optical detection system, but will mainly include a cross-junction connected to a lab-view pneumatically actuated valve. Additional pneumatic actuated branches can be employed to improve the sorting efficiency and obtain precise droplets for downstream PCR testing and sequencing or cyclic evolutionary studies (Figure 3.1).

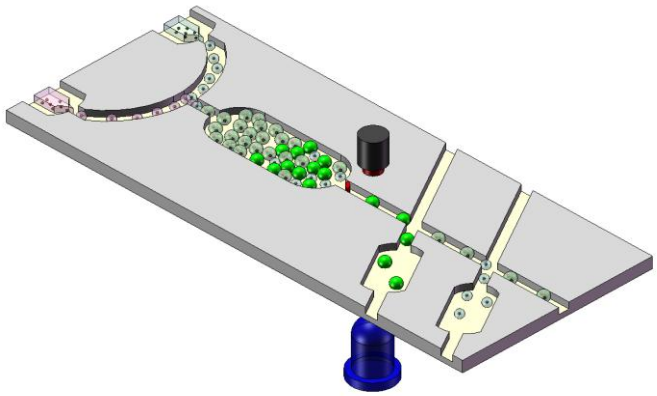

Figure 3.1. 3D model evolutionary microbial co-culture device. Optical detection model for microdroplet detection and sorting a LED/PMT and pneumatic actuation system.

3.2.4 Microbial Evolutionary Studies

Lastly, as mentioned previously a fully functional microdroplet system will be used to characterize rare growth or mutation in sets of co-cultured microbes that are naturally present in the environment. Considering that in some cases this may include select agents that are somewhat dangerous to humans, the device can provide an additional barrier for researchers to prevent exposure of such agents. In addition this device can provide the foundation for future workings including a fully functional microdroplet microbial culture, microdroplet PCR, and microdroplet sequencing platform that can almost eliminate exposure risks, while reducing reagent consumption and keeping a high-throughput system.

REFERENCES

[1] Song, H., D. L. Chen, et al. (2006). "Reactions in droplets in microfluidic channels." Angewandte Chemie International Edition **45**(44): 7336-7356.

[2] Baroud, C. N., F. Gallaire, et al. (2010). "Dynamics of microfluidic droplets." Lab on a Chip **10**(16): 2032-2045.

[3] Theberge, A. B., F. Courtois, et al. (2010). "Microdroplets in microfluidics: an evolving platform for discoveries in chemistry and biology." Angewandte Chemie International Edition **49**(34): 5846-5868.

[4] Zhang, K., Q. Liang, et al. (2011). "On-demand microfluidic droplet manipulation using hydrophobic ferrofluid as a continuous-phase." Lab on a Chip **11**(7): 1271-1275.

[5] Pekin, D., Y. Skhiri, et al. (2011). "Quantitative and sensitive detection of rare mutations using droplet-based microfluidics." Lab on a Chip **11**(13): 2156-2166.

[6] Boedicker, J. Q., L. Li, et al. (2008). "Detecting bacteria and determining their susceptibility to antibiotics by stochastic confinement in nanoliter droplets using plug-based microfluidics." Lab on a Chip **8**(8): 1265-1272.

[7] Huebner, A., S. Sharma, et al. (2008). "Microdroplets: a sea of applications?" Lab on a Chip **8**(8): 1244-1254.

[8] Teh, S.-Y., R. Lin, et al. (2008). "Droplet microfluidics." Lab on a Chip **8**(2): 198-220.

[9] Hsiung, S.-K. and et al. (2006). "Micro-droplet formation utilizing microfluidic flow focusing and controllable moving-wall chopping techniques." Journal of Micromechanics and Microengineering **16**(11): 2403.

[10] Lai, C.-W., Y.-H. Lin, et al. (2008). "A microfluidic chip for formation and collection of emulsion droplets utilizing active pneumatic micro-choppers and micro-switches." Biomedical Microdevices **10**(5): 749-756.

[11] Cheng-Tso, C. and L. Gwo-Bin (2006). "Formation of microdroplets in liquids utilizing active pneumatic choppers on a microfluidic chip." Microelectromechanical Systems, Journal of **15**(6): 1492-1498.

[12] Yen-Heng, L., L. Chun-Hong, et al. (2008). "Droplet formation utilizing controllable moving-wall structures for double-emulsion applications." Microelectromechanical Systems, Journal of **17**(3): 573-581.

[13] Lin, Y.-H., C.-T. Chen, et al. (2007). "Multiple-channel emulsion chips utilizing pneumatic choppers for biotechnology applications." Biomedical Microdevices **9**(6): 833-843.

[14] Kim, S. J., Y.-A. Song, et al. (2006). "Electrohydrodynamic generation and delivery of monodisperse picoliter droplets using a poly(dimethylsiloxane) Microchip." Analytical Chemistry **78**(23): 8011-8019.

[15] Glawdel, T., C. Elbuken, et al. (2012). "Droplet formation in microfluidic T-junction generators operating in the transitional regime. I. Experimental observations." Physical Review E **85**(1): 016322.

[16] Glawdel, T., C. Elbuken, et al. (2012). "Droplet formation in microfluidic T-junction generators operating in the transitional regime. II. Modeling." Physical Review E **85**(1): 016323.

[17] Atencia, J. and D. J. Beebe (2005). "Controlled microfluidic interfaces." Nature **437**(7059): 648-655.

[18] Gu, H., M. H. G. Duits, et al. (2011). "Droplets formation and merging in two-phase flow microfluidics." International Journal of Molecular Sciences **12**(4): 2572-2597.

[19] Shui, L., A. van den Berg, et al. (2009). "Interfacial tension controlled W/O and O/W 2-phase flows in microchannel." Lab on a Chip **9**(6): 795-801.

[20] Lai, J.-M. and et al. (2010). "Influence of liquid hydrophobicity and nozzle passage curvature on microfluidic dynamics in a drop ejection process." Journal of Micromechanics and Microengineering **20**(1): 015033.

[21] Tan, S.-H. and et al. (2010). "Formation and manipulation of ferrofluid droplets at a microfluidic T -junction." Journal of Micromechanics and Microengineering **20**(4): 045004.

[22] Say-Hwa, T., N. Nam-Trung, et al. (2010). "Formation and manipulation of ferrofluid droplets at a microfluidic T -junction." Journal of Micromechanics and Microengineering **20**(4): 045004.

[23] Wang, W., R. Xie, et al. (2011). "Controllable microfluidic production of multicomponent multiple emulsions." Lab on a Chip **11**(9): 1587-1592.

[24] Torii, T. (2010). “Droplet handling nano/micro biotechnology.” I. Endo and T. Nagamune, Springer Berlin / Heidelberg. **119**: 165-177.

[25] Wu, N., Y. Zhu, et al. (2007). “Effects of surfactants on the formation of microdroplets in the flow focusing microfluidic device.” Canberra, ACT, Australia, SPIE. **6799:** 67990C.

[26] Rondeau, E. and J. J. Cooper-White (2008). "Biopolymer microparticle and nanoparticle formation within a microfluidic device." Langmuir **24(**13): 6937-6945.

[27] Huang, K.-S., K. Lu, et al. (2009). "Microfluidic controlling monodisperse microdroplet for 5-fluorouracil loaded genipin-gelatin microcapsules." Journal of Controlled Release **137**(1): 15-19.

[28] Seiffert, S. and D. A. Weitz (2010). "Controlled fabrication of polymer microgels by polymer-analogous gelation in droplet microfluidics." Soft Matter **6**(14): 3184-3190.

[29] Lee, D. H., W. Lee, et al. (2011). “On-chip gelation of temporally controlled alginate microdroplets.” Solid-State Sensors, Actuators and Microsystems Conference (TRANSDUCERS), 2011 16th International: 234-237.

[30] Bai, Y., X. He, et al. (2010). "A double droplet trap system for studying mass transport across a droplet-droplet interface." Lab on a Chip **10**(10): 1281-1285.

[31] Sgro, A. E. and D. T. Chiu (2010). "Droplet freezing, docking, and the exchange of immiscible phase and surfactant around frozen droplets." Lab on a Chip **10**(14): 1873-1877.

[32] Hufnagel, H., A. Huebner, et al. (2009). "An integrated cell culture lab on a chip: modular microdevices for cultivation of mammalian cells and delivery into microfluidic microdroplets." Lab on a Chip **9**(11): 1576-1582.

[33] Courtois, F., L. F. Olguin, et al. (2009). "Controlling the retention of small molecules in emulsion microdroplets for use in cell-based assays." Analytical Chemistry **81**(8): 3008-3016.

[34] Brouzes, E., M. Medkova, et al. (2009). "Droplet microfluidic technology for single-cell high-throughput screening." Proceedings of the National Academy of Sciences **106**(34): 14195-14200.

[35] Mazutis, L., J.-C. Baret, et al. (2009). "A fast and efficient microfluidic system for highly selective one-to-one droplet fusion." Lab on a Chip **9**(18): 2665-2672.

[36] Hong, J., M. Choi, et al. (2010). "Passive self-synchronized two-droplet generation." Lab on a Chip **10**(20): 2702-2709.

[37] Im, D. J., J. Noh, et al. (2011). "Electrophoresis of a charged droplet in a dielectric liquid for droplet actuation." Analytical Chemistry **83**(13): 5168-5174.

[38] Wang, K., Y. Lu, et al. (2012). "Microdroplet coalescences at microchannel junctions with different collision angles." AIChE Journal.

[39] Bremond, N., A. R. Thiam, et al. (2008). "Decompressing Emulsion Droplets Favors Coalescence." Physical Review Letters **100**(2): 024501.

[40] Lai, A. N. N., N. Bremond, et al. (2009). "Separation-driven coalescence of droplets: an analytical criterion for the approach to contact." Journal of Fluid Mechanics **632**: 97-107.

[41] Gunther, A. and K. F. Jensen (2006). "Multiphase microfluidics: from flow characteristics to chemical and materials synthesis." Lab on a Chip **6**(12): 1487-1503.

[42] Fidalgo, L. M., C. Abell, et al. (2007). "Surface-induced droplet fusion in microfluidic devices." Lab on a Chip **7**(8): 984-986.

[43] Li, Z. G., K. Ando, et al. (2011). "Fast on-demand droplet fusion using transient cavitation bubbles." Lab on a Chip **11**(11): 1879-1885.

[44] Dixit, S. S., H. Kim, et al. (2010). "Light-driven formation and rupture of droplet bilayers." Langmuir **26**(9): 6193-6200.

[45] Zagnoni, M., G. Le Lain, et al. (2010). "Electrocoalescence mechanisms of microdroplets using localized electric fields in microfluidic channels." Langmuir **26**(18): 14443-14449.

[46] Park, J., A. Kerner, et al. (2011). "Microdroplet-enabled highly parallel co-cultivation of microbial communities." PLoS ONE **6**(2): e17019.

[47] Abate, A. R., T. Hung, et al. (2010). "High-throughput injection with microfluidics using picoinjectors." Proceedings of the National Academy of Sciences **107**(45): 19163-19166.

[48] Szymborski, T., P. M. Korczyk, et al. (2011). "Ionic polarization of liquid-liquid interfaces; dynamic control of the rate of electro-coalescence." Applied Physics Letters **99**(9): 094101-094103.

[49] Zagnoni, M. and J. M. Cooper (2010). "A microdroplet-based shift register." Lab on a Chip **10**(22): 3069-3073.

[50] Harada, Y., Y. Dong Hyun, et al. (2012). “Size-oriented passive droplet sorting by using surface free energy with micro guide groove.” Micro Electro Mechanical Systems (MEMS) IEEE 25th International Conference: 1105 - 1108.

[51] Joensson, H. N., M. Uhlen, et al. (2011). "Droplet size based separation by deterministic lateral displacement-separating droplets by cell-induced shrinking." Lab on a Chip **11**(7): 1305-1310.

[52] Tan, Y.-C., J. S. Fisher, et al. (2004). "Design of microfluidic channel geometries for the control of droplet volume, chemical concentration, and sorting." Lab on a Chip **4**(4): 292-298.

[53] deMello, A. J. (2006). "Control and detection of chemical reactions in microfluidic systems." Nature **442**(7101): 394-402.

[54] Jungwoo, L., C. Jin Ho, et al. (2011). "Backscattering measurement from a single microdroplet." Ultrasonics, Ferroelectrics and Frequency Control, IEEE Transactions on **58**(4): 874-879.

[55] Beer, N. R., K. A. Rose, et al. (2009). "Monodisperse droplet generation and rapid trapping for single molecule detection and reaction kinetics measurement." Lab on a Chip **9**(6): 841-844.

[56] Chabert, M., K. D. Dorfman, et al. (2006). "Automated microdroplet platform for sample manipulation and polymerase chain reaction." Analytical Chemistry **78**(22): 7722-7728.

[57] Huebner, A., D. Bratton, et al. (2009). "Static microdroplet arrays: a microfluidic device for droplet trapping, incubation and release for enzymatic and cell-based assays." Lab on a Chip **9**(5): 692-698.

[58] Park, S., P. M. Wolanin, et al. (2003). "Influence of topology on bacterial social interaction." Proceedings of the National Academy of Sciences of the United States of America **100**(24): 13910-13915.

[59] Lee, K. G., T. J. Park, et al. (2010). "Synthesis and utilization of E. coli-encapsulated PEG-based microdroplet using a microfluidic chip for biological application." Biotechnology and Bioengineering **107**(4): 747-751.

[60] Wu, N., Y. Zhu, et al. (2009). "A PMMA microfluidic droplet platform for in vitro protein expression using crude E. coli S30 extract." Lab on a Chip **9**(23): 3391-3398.

[61] Abbyad, P., P.-L. Tharaux, et al. (2010). "Sickling of red blood cells through rapid oxygen exchange in microfluidic drops." Lab on a Chip **10**(19): 2505-2512.

[62] Ashok, P. C., G. P. Singh, et al. (2011). "Waveguide confined raman spectroscopy for microfluidic interrogation." Lab on a Chip **11**(7): 1262-1270.

[63] Binz, M., A. P. Lee, et al. (2010). "Motility of bacteria in microfluidic structures." Microelectronic Engineering **87**(5–8): 810-813.

[64] Cecchini, M. P., J. Hong, et al. (2011). "Ultrafast surface enhanced resonance raman scattering detection in droplet-based microfluidic systems." Analytical Chemistry **83**(8): 3076-3081.

[65] Chen, C.-H., A. Sarkar, et al. (2011). "Enhancing protease activity assay in droplet-based microfluidics using a biomolecule concentrator." Journal of the American Chemical Society **133**(27): 10368–10371.

[66] Chen, D., W. Du, et al. (2008). "The chemistrode: a droplet-based microfluidic device for stimulation and recording with high temporal, spatial, and chemical resolution." Proceedings of the National Academy of Sciences **105**(44): 16843-16848.

[67] Chen, D. L., L. Li, et al. (2007). "Using three-phase flow of immiscible liquids to prevent coalescence of droplets in microfluidic channels: criteria to identify the third liquid and validation with protein crystallization." Langmuir **23**(4): 2255-2260.

[68] Damean, N., L. F. Olguin, et al. (2009). "Simultaneous measurement of reactions in microdroplets filled by concentration gradients." Lab on a Chip **9**(12): 1707-1713.

[69] Frenz, L., K. Blank, et al. (2009). "Reliable microfluidic on-chip incubation of droplets in delay-lines." Lab on a Chip **9**(10): 1344-1348.

[70] Grigoriev, R. O., M. F. Schatz, et al. (2006). "Chaotic mixing in microdroplets." Lab on a Chip **6**(10): 1369-1372.

[71] Hatch, A. C., J. S. Fisher, et al. (2011). "Tunable 3D droplet self-assembly for ultra-high-density digital micro-reactor arrays." Lab on a Chip **11**(15): 2509-2517.

[72] Hatch, A. C., J. S. Fisher, et al. (2011). "1-Million droplet array with wide-field fluorescence imaging for digital PCR." Lab on a Chip **11**(22): 3838-3845.

[73] Held, M., A. P. Lee, et al. (2010). "Microfluidics structures for probing the dynamic behaviour of filamentous fungi." Microelectronic Engineering **87**(5–8): 786-789.

[74] Hsieh, A. T.-H., N. Hori, et al. (2009). "Nonviral gene vector formation in monodispersed picolitre incubator for consistent gene delivery." Lab on a Chip **9**(18): 2638-2643.

[75] Hua, Z., J. L. Rouse, et al. (2010). "Multiplexed real-time polymerase chain reaction on a digital microfluidic platform." Analytical Chemistry **82**(6): 2310-2316.

[76] Ji, X.-H., W. Cheng, et al. (2011). "On-demand preparation of quantum dot-encoded microparticles using a droplet microfluidic system." Lab on a Chip.

[77] Kirkness, E. F. (2009). "Targeted sequencing with microfluidics." Nat Biotech **27**(11): 998-999.

[78] Lambert, G., L. Estévez-Salmeron, et al. (2011). "An analogy between the evolution of drug resistance in bacterial communities and malignant tissues." Nat Rev Cancer **11**(5): 375-382.

[79] Martino, C., M. Zagnoni, et al. (2011). "Intracellular protein determination Using droplet-based immunoassays." Analytical Chemistry **83**(13): 5361-5368.

[80] Mazutis, L., J.-C. Baret, et al. (2009). "Multi-step microfluidic droplet processing: kinetic analysis of an in vitro translated enzyme." Lab on a Chip **9**(20): 2902-2908.

[81] Piggee, C. (2008). "Single-copy PCR in uniform nanoliter droplets." Analytical Chemistry **80**(11): 3946-3946.

[82] Shen, A. Q., D. Wang, et al. (2007). "Kinetics of colloidal templating using emulsion drop consolidation." Langmuir **23**(26): 12821-12826.

[83] Shim, J.-u., L. F. Olguin, et al. (2009). "Simultaneous determination of gene expression and enzymatic activity in individual bacterial cells in microdroplet compartments." Journal of the American Chemical Society **131**(42): 15251-15256.

[84] Shim, J.-u., S. N. Patil, et al. (2011). "Controlling the contents of microdroplets by exploiting the permeability of PDMS." Lab on a Chip **11**(6): 1132-1137.

[85] Srisa-Art, M., A. J. deMello, et al. (2007). "High-throughput DNA droplet assays using picoliter reactor volumes." Analytical Chemistry **79**(17): 6682-6689.

[86] Tewhey, R., J. B. Warner, et al. (2009). "Microdroplet-based PCR enrichment for large-scale targeted sequencing." Nat Biotech **27**(11): 1025-1031.

[87] Wang, W., C. Yang, et al. (2009). "On-demand microfluidic droplet trapping and fusion for on-chip static droplet assays." Lab on a Chip **9**(11): 1504-1506.

[88] Zeng, Y., R. Novak, et al. (2010). "High-performance single cell genetic analysis using microfluidic emulsion generator arrays." Analytical Chemistry **82**(8): 3183-3190.

APPENDIX A

MASK DESIGN: MICRODROPLET CULTURE DEVICE

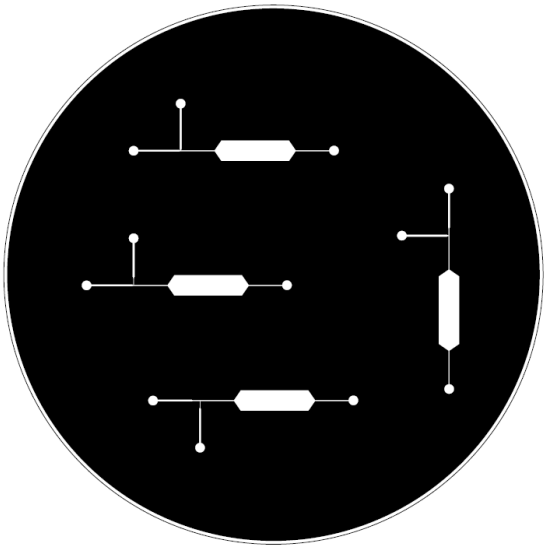

Figure A.1. Mask layout of microdroplet culture device.

MASK DESIGN: MULTI-VALVE MULTI-CHAMBER MICRODROPLET CULTURE DEVICE

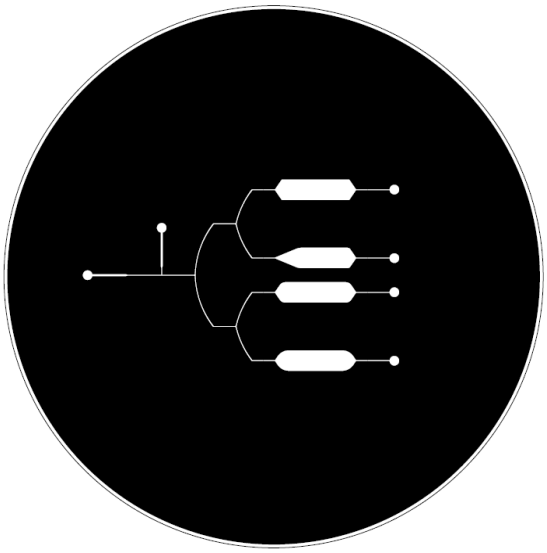

Figure A.2. Mask layout of multi-chamber layer.

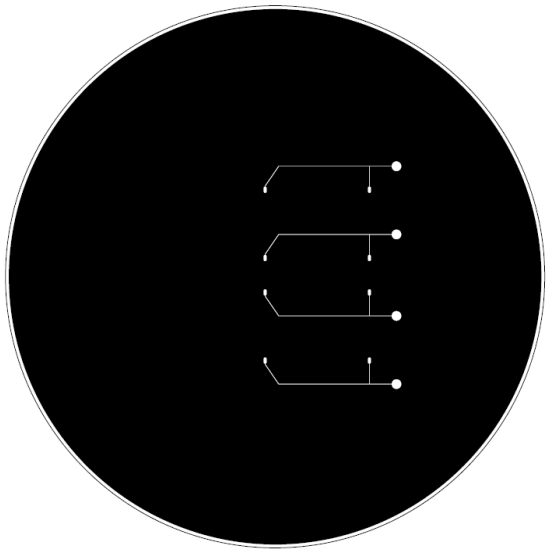

Figure A.3. Mask layout of multi-valve layer.

MASK DESIGN: RAILROAD-LIKE SYNCHRONIZATION DEVICE

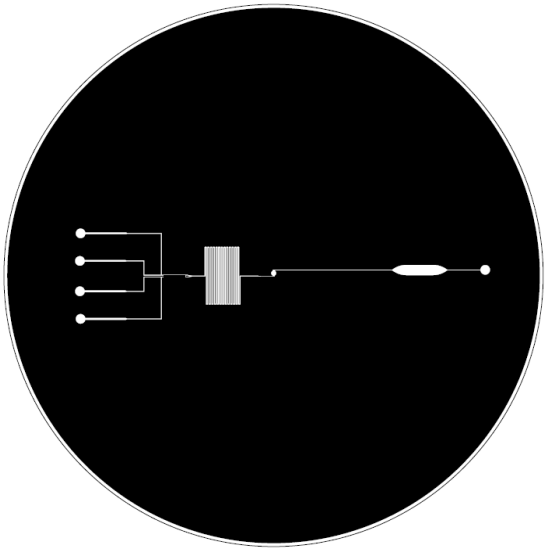

Figure A.4. Mask layout of railroad-like synchronization.

MASK DESIGN: OSCILLATOR AND REGULATOR SYNCHRONIZATION DEVICE

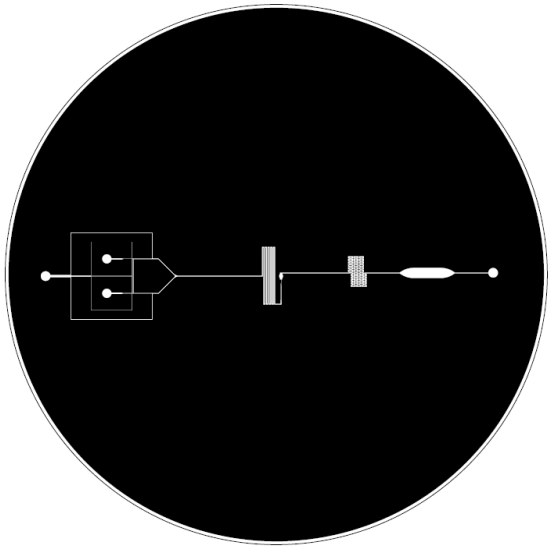

Figure A.5. Mask layout of oscillator/regulator synchronization.

MASK DESIGN: WIDENED-NARROWED MERGING DEVICE AND PILLAR ARRAY MERGING DEVICE

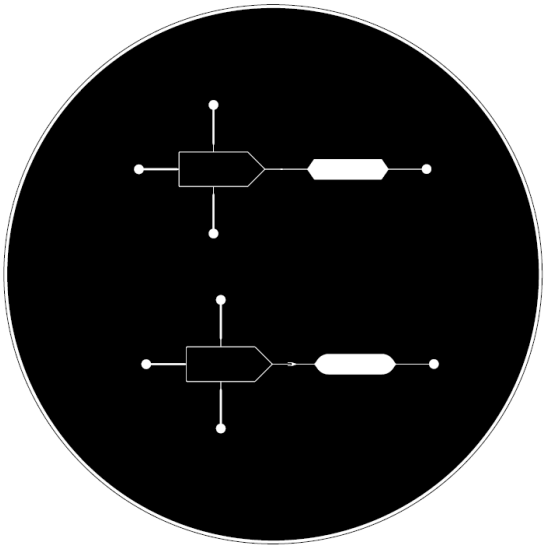

Figure A.6. Mask layout of passive merging: narrow/widening and pillar array.

MASK DESIGN: FIRST GENERATION ELECTROCOALESCENCE DEVICES

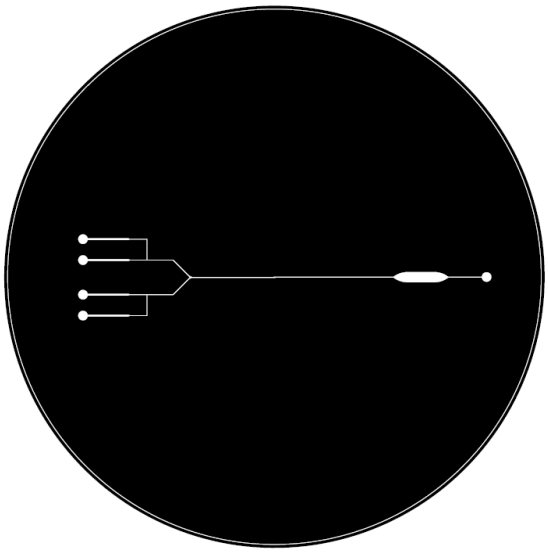

Figure A.7. Mask layout of 250 µm electrocoalescence chamber.

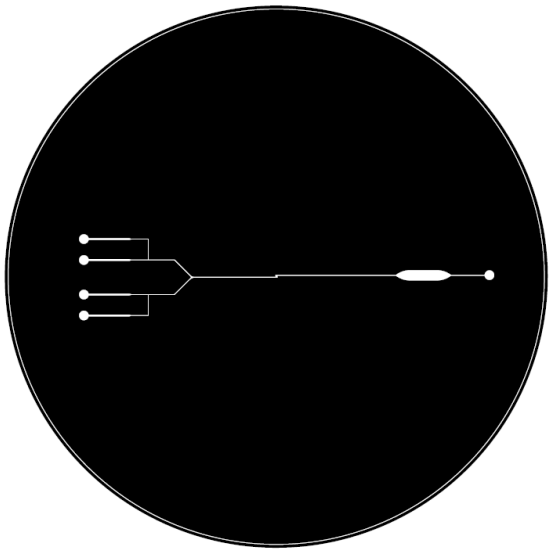

Figure A.8. Mask layout of 500 µm electrocoalescence chamber.

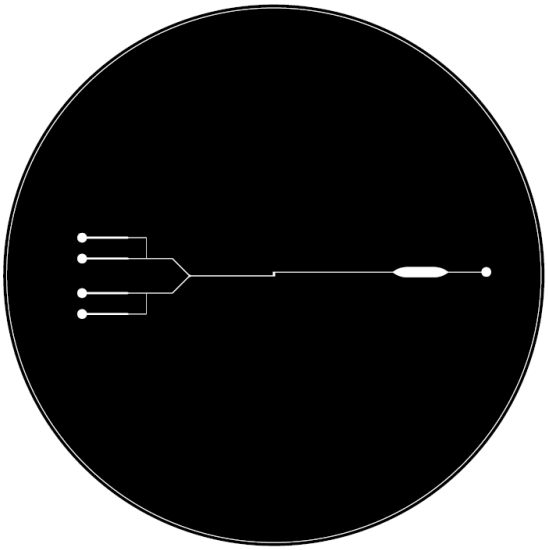

Figure A.9. Mask layout of 750 µm electrocoalescence chamber.

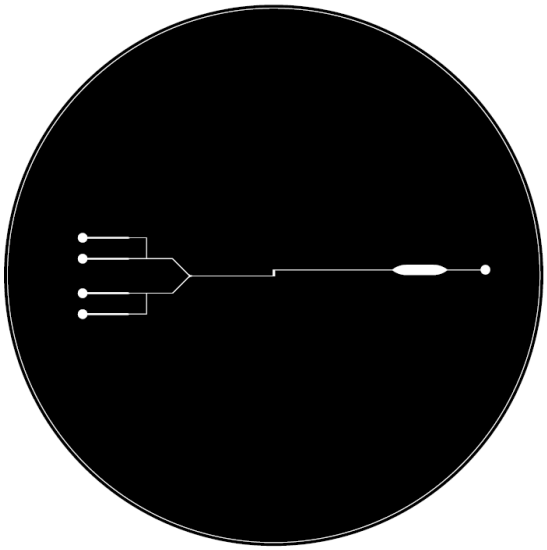

Figure A.10. Mask layout of 1000 µm electrocoalescence chamber.

MASK DESIGN: SECOND GENERATION ELECTROCOALESCENCE DEVICES

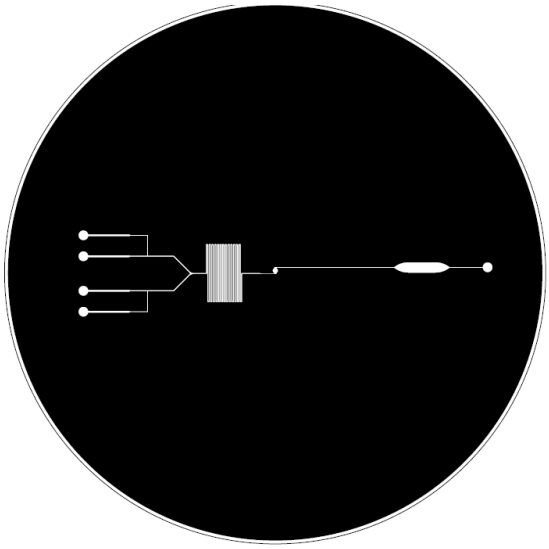

Figure A.11. Mask layout of oval shape electrocoalescence chamber.

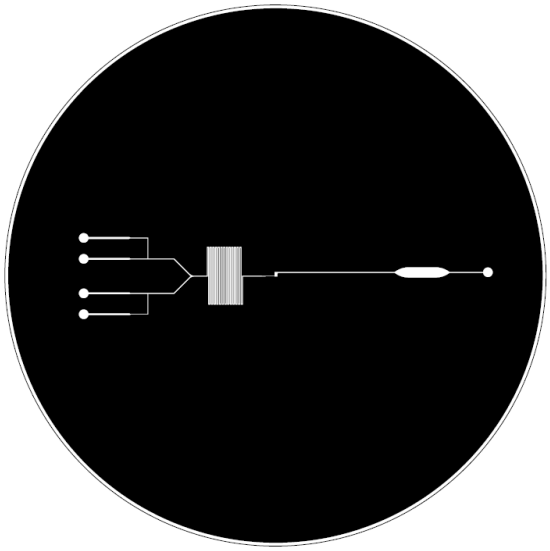

Figure A.12. Mask layout of narrowed/widened/narrowed electrocoalescence chamber.

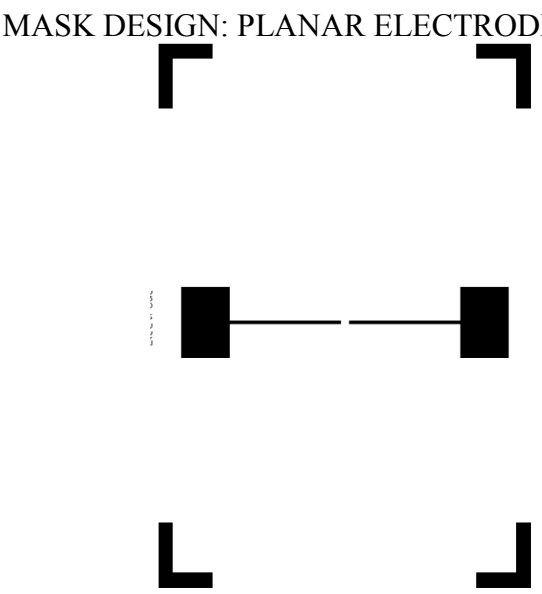

Figure A.13. Mask layout of planar/dual co-planar/3D electrodes.

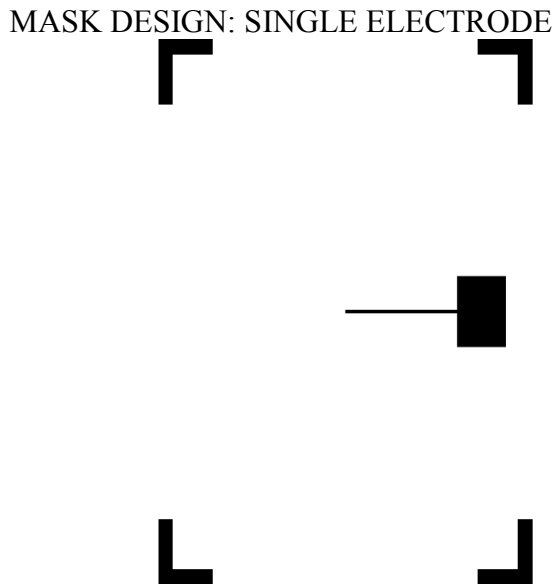

Figure A.14. Mask layout of co-planar electrode.

MASK DESIGN: 3D ELECTROCOALESCENCE DEVICE

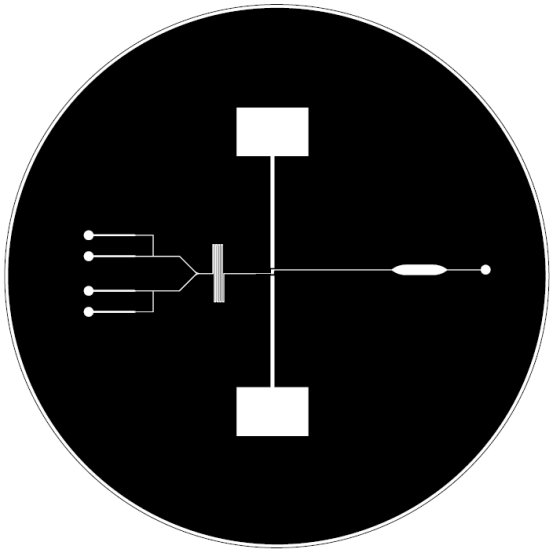

Figure A.15. Mask layout of 3D electrocoalescence.

APPENDIX B

MASTER FABRICATION PROCEDURE

B.1. Electrode Patterning Procedure

1. Clean the 2x3 inch glass slide with acetone, IPA, and DI water in sequence and dry with N2 gas

2. Dehydrate baking at 200°C for 10 minutes

3. Deposit Cr/Cu layer using an E-beam evaporator to a thickness of 2000 Å

4. Repeat steps 1 and 2

5. Spin coat Microposit S1818 photoresist (Rohm and Haas Electronic Material LLC, Marlborough, MA) on the glass slide at 4000 rpm for 30 seconds with an acceleration time of 5 seconds

6. Soft baking at 95°C for 10 minutes, cool down

7. Expose UV using a mask electrode design (MJB3, SUSS MicroTec Inc., Waterbury Center, VT) at 12 mW/cm2 (wavelength: 320 nm) for 14 second

8. Develop the pattern using MF-319 developer (Rohm and Haas Electronic Material LLC, Marlborough, MA) for 20-40 seconds

9. Rinse in DI water and dry with N2 gas. Only the electrodes were covered with photoresist

10. Etch uncovered Copper with Copper etchant for about 30 seconds

11. Rinse with DI water

12. Etch uncovered Chromium with Chromium etchant for about 30 seconds

13. Rinse the glass slide with DI water, acetone, IPA, and DI water in sequence, and dry with N2 gas

B.2. Fluidic Channel Layer Master Fabrication Procedure

1. Rinse the silicon wafer with acetone, IPA, and DI water in sequence, and dry with N2 gas

2. Dehydrate baking at 200°C for 10 minutes

3. Spin coat 100 μm thick photoresist (SU-8TM 2050, Microchem, Inc., Newton, MA) on the silicon wafer at 1300 rpm for 40 seconds

4. Soft baking at 65°C for 10 minutes, followed by 95°C baking for 45 minutes, cool down

5. Expose UV using a fluidic channel layer mask (MA6, SUSS MicroTec Inc., Waterbury Center, VT) at 120 mJ/cm2

6. Post exposure bake at 65°C for 10 minutes, followed by 95°C baking for 40 minutes, cool down

7. Develop the patterns using Microposit Thinner Type P (Shipley Co., Marlborough, MA) for about 5 seconds

8. Rinse with IPA and DI water, and dry with N2 gas

B.3. Pneumatic Layer Master Fabrication Procedure

1. Rinse a bare 3 inch silicon wafer with acetone, IPA, and DI water in sequence, and dry with N2 gas

2. Dehydrate baking at 200°C for 10 minutes

3. Spin coat 120 μm thick photoresist (SU-8TM 2050, Microchem, Inc., Newton, MA) on the silicon wafer at 800 rpm for 40 seconds

4. Soft baking at 65°C for 10 minutes, followed by 95°C baking for 45 minutes, cool down

5. Expose UV using a pneumatic layer mask (MA6, SUSS MicroTec Inc., Waterbury Center, VT) at 250 mJ/cm2

6. Post exposure bake at 65°C for 10 minutes, followed by 95°C baking for 40 minutes, cool down

7. Develop the patterns using Microposit Thinner Type P (Shipley Co., Marlborough, MA) for about 5 minutes

8. Rinse with IPA and DI water, and dry with N2 gas

APPENDIX C

PDMS DEVICE FABRICATION PROCEDURE

C.1. Thick Fluidic Channel Layer PDMS Fabrication Procedure

1. Place the fabricated fluidic channel layer master mold wafers inside the desiccator together with a weight boat containing 6 ~ 7 drops of tridecafluoro-1,1,2,2-tetrahydrooctyl (trichlorosilane, United Chemical Technologies, Inc., Bristol, PA)
2. Vacuum the desiccator for 10 min to allow trichlorosilane vaporization and evenly sprayed over the wafers
3. Mix PDMS (Sylgard® 184, Dow Corning, Inc., Midland, MI) prepolymer with curing agent at 10 : 1 ratio, and degas in a desiccator for 10 minutes
4. Pour the degassed PDMS prepolymer mixture onto trichlorosilane coated master wafers for 20 g per 3 inch wafer, and degas again in the desiccator for 30 min
5. Cure in an 85°C oven for 2 h

C.2. Pneumatic Layer PDMS Block Fabrication Procedure

1. Place the fabricated pneumatic layer master mold wafers inside the desiccator together with a weight boat containing 6 ~ 7 drops of tridecafluoro-1,1,2,2-tetrahydrooctyl (trichlorosilane, United Chemical Technologies, Inc., Bristol, PA)
2. Vacuum the desiccator for 10 min to allow trichlorosilane vaporization and evenly sprayed over the wafers
3. Mix PDMS (Sylgard® 184, Dow Corning, Inc., Midland, MI) prepolymer with curing agent at 10 : 1 ratio, and degas in a desiccator for 10 minutes

4. Pour the degassed PDMS prepolymer mixture onto trichlorosilane coated master wafers for 20 g per 3 inch wafer, and degas again in the desiccator for 30 min

5. Cure in an 85°C oven for 2 hours

C.3. Multi-valve Multi-chamber PDMS Device Bonding

1. Peel off the cured PDMS fluidic layer membrane and pneumatic layer block

2. Punch holes in the pneumatic layer block with a gauge 19 needle

3. Open via holes on the fluidic layer membrane with a sharp tweezer

4. Apply oxygen plasma treatment (100 mTorr, 100W, 40 sec) for both fluidic layer membrane and pneumatic layer block, visually align under a stereo microscope

5. Bake at 80°C on a hotplate for 8 h

C.4. Electrocoalescence-PDMS Device Bonding

1. Peel off the cured PDMS fluidic layer membrane

2. Apply oxygen plasma treatment (100 mTorr, 100W, 40sec) for the top of the fluidic layer membrane and plain PDMS blocks

3. Bond the blocks on top of the inlet and outlets of the PDMS channel layer

4. Punch holes in the PDMS channel layer through the PDMS blocks using a gauge 19 needle

5. Apply oxygen plasma treatment (100 mTorr, 100W, 40 sec) for both fluidic layer and previously spin coated glass electrode (3000rpm, 40sec), apply methanol and align under stereoscope

6. Bake at 80°C on a hotplate for 8 h

7. (Optional: for co-planar and dual co-planar devices) Oxygen plasma treat (100 mTorr, 100W, 40sec) the top of the PDMS channel layer membrane and another previously spin coated (3000rpm, 40sec) glass electrode, apply methanol if needed and align using stereoscope

8. Bake at 80°C on a hotplate for 8 h

APPENDIX D

FUNCTION GENERATOR / MOS-FET / DC POWER SUPPLY FOR ELECTRIC FIELD INDUCTION IN MICRODROPLET MERGING CHAMBER

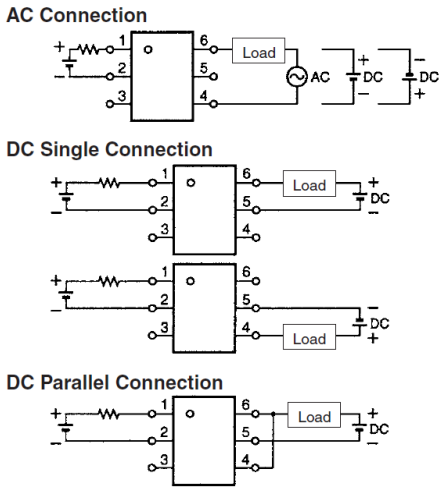

D.1. Schematic of mos-fet relay circuit. Mos-fet relay circuit reproduced from Omron® device operation data sheet. (The configuration used in all of these experiments was the first "DC Signal Connection" schematic.)

COMSOL SIMULATIONS

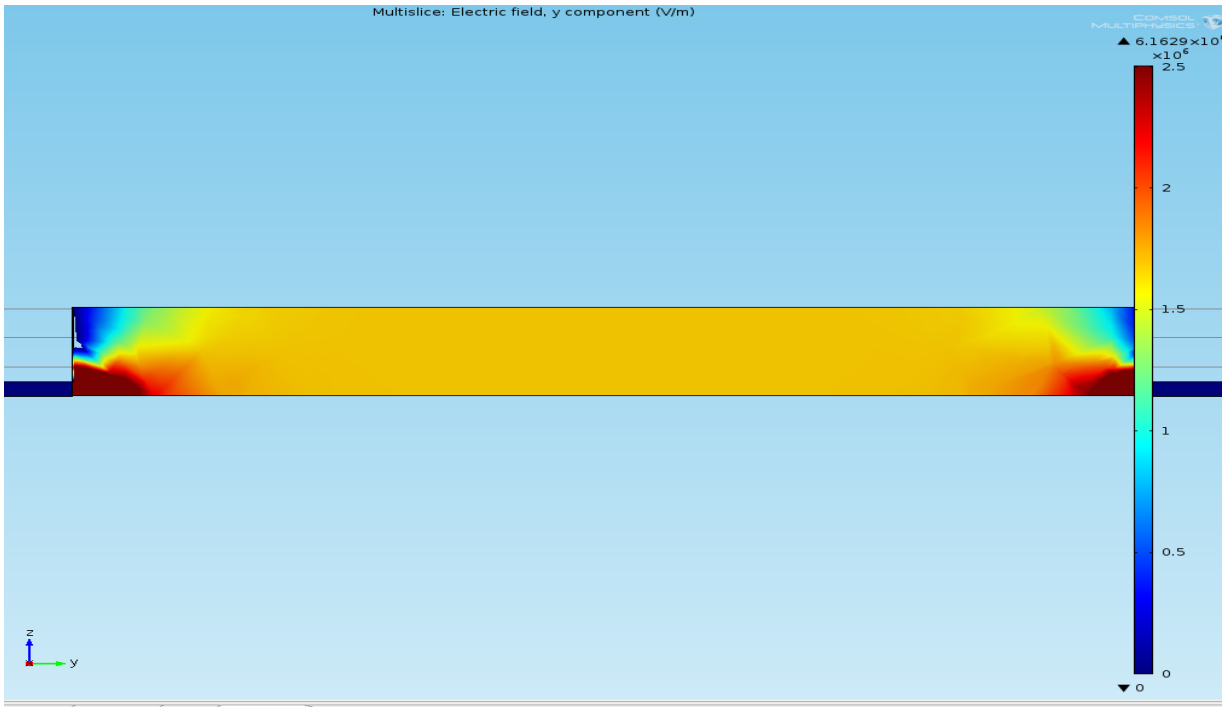

D.2. Comsol model of planar electrocoalescence design.

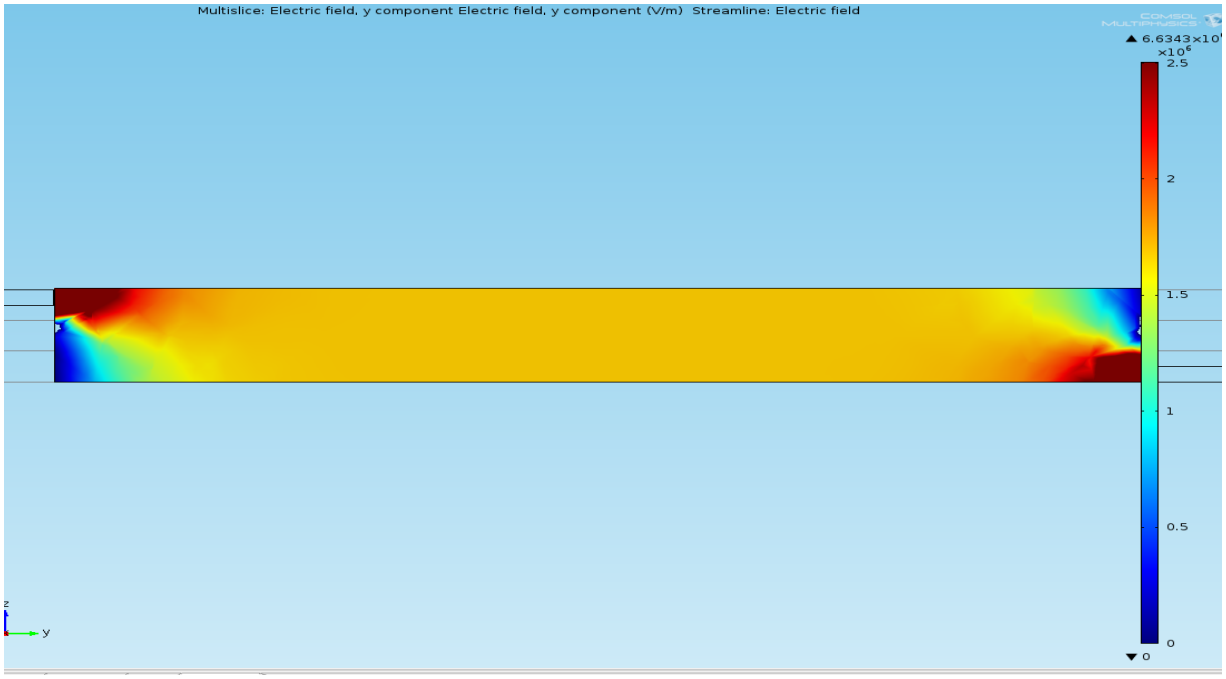

D.3. Comsol model of co-planar electrocoalescence design.

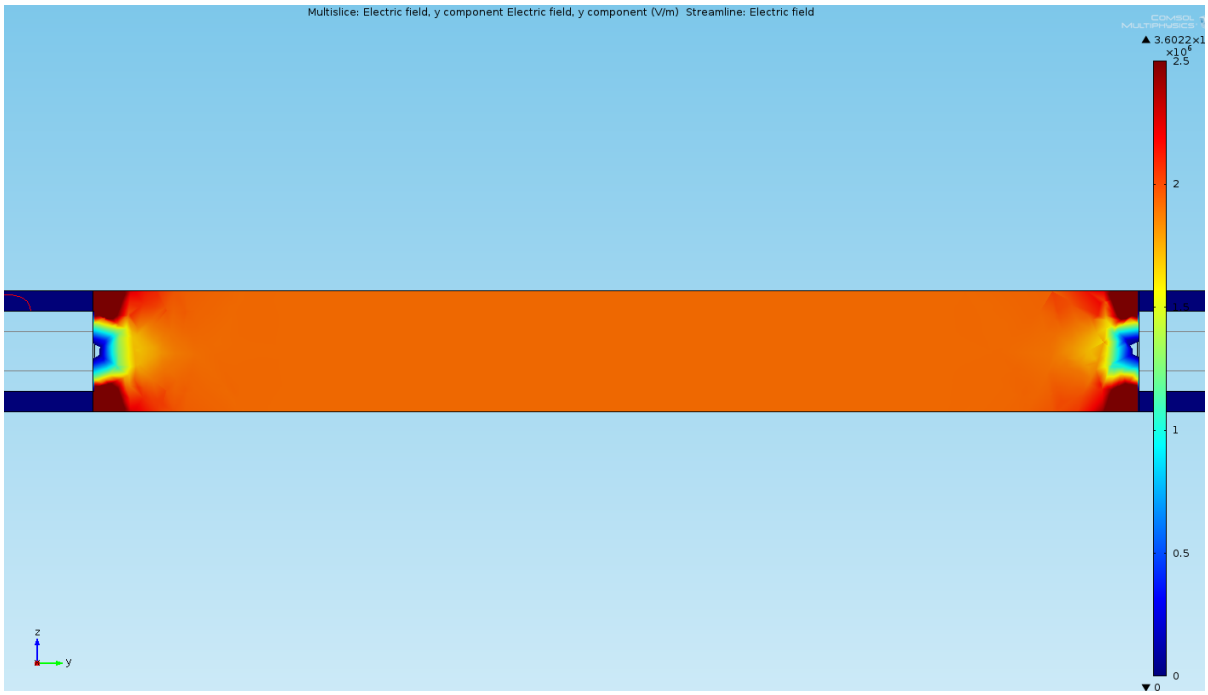

D.4. Comsol model of dual-planar electrocoalescence design.

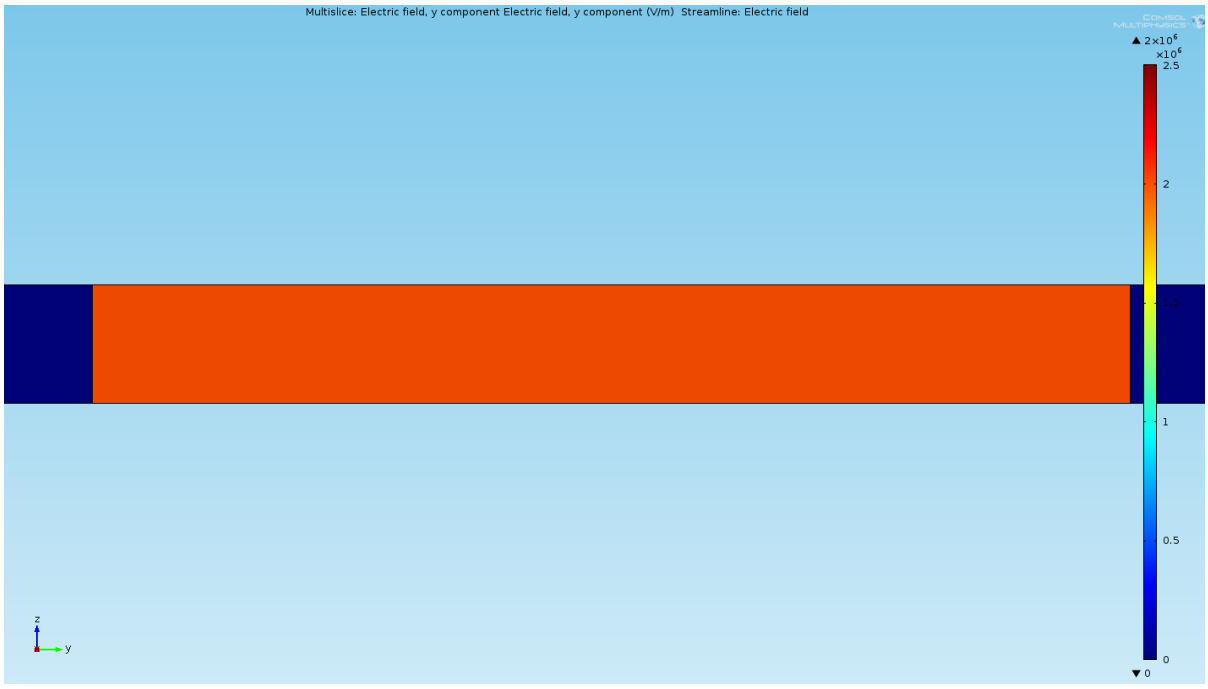

D.5. Comsol model of 3D electrocoalescence design.

VITA

Name:	Adrian Ryan Guzman
Address:	Zachry Engineering Center, Mailstop 3128 TAMU, College Station, TX 77843
Email Address:	adrianrg74@gmail.com, adrianrg74@tamu.edu
Education:	B.S., Biomedical Engineering, Texas A&M University College Station, 2008